Aurora kinase A-specific T-cell receptor gene transfer redirects T lymphocytes to display effective antileukemia reactivity

*Kozo Nagai,[1] *Toshiki Ochi,[1] Hiroshi Fujiwara,[1,2] Jun An,[1] Toshiaki Shirakata,[1] Junichi Mineno,[3] Kiyotaka Kuzushima,[4] Hiroshi Shiku,[5] J. Joseph Melenhorst,[6] Emma Gostick,[7] David A. Price,[7] Eiichi Ishii,[8] and Masaki Yasukawa[1,2]

[1]Department of Bioregulatory Medicine, Ehime University Graduate School of Medicine, Ehime, Japan; [2]Department of Cell Growth and Cancer Regulation, Ehime University Proteomedicine Research Center, Ehime, Japan; [3]Takara Bio Inc Center for Cell and Gene Therapy, Shiga, Japan; [4]Division of Immunology, Aichi Cancer Center, Aichi, Japan; [5]Department of Cancer Vaccine and Immuno-Gene Therapy, Mie University Graduate School of Medicine, Mie, Japan; [6]Hematology Branch, National Heart, Lung, and Blood Institute, National Institutes of Health, Bethesda, MD; [7]Department of Infection, Immunity and Biochemistry, Cardiff University School of Medicine, Cardiff, United Kingdom; and [8]Department of Pediatrics, Ehime University Graduate School of Medicine, Ehime, Japan

Aurora kinase A (AURKA) is overexpressed in leukemias. Previously, we demonstrated that AURKA-specific CD8$^+$ T cells specifically and selectively lysed leukemia cells, indicating that AURKA is an excellent target for immunotherapy. In this study, we examined the feasibility of adoptive therapy using redirected T cells expressing an HLA-A*0201–restricted AURKA$_{207-215}$-specific T-cell receptor (TCR). Retrovirally transduced T cells recognized relevant peptide-pulsed but not control target cells. Furthermore, TCR-redirected CD8$^+$ T cells lysed AURKA-overexpressing human leukemic cells in an HLA-A*0201–restricted manner, but did not kill HLA-A*0201$^+$ normal cells, including hematopoietic progenitors. In addition, AURKA$_{207-215}$-specific *TCR*-transduced CD4$^+$ T cells displayed target-responsive Th1 cytokine production. Finally, AURKA$_{207-215}$-specific *TCR*-transduced CD8$^+$ T cells displayed antileukemia efficacy in a xenograft mouse model. Collectively, these data demonstrate the feasibility of redirected T cell–based AURKA-specific immunotherapy for the treatment of human leukemia. (*Blood*. 2012;119(2):368-376)

Introduction

Aurora kinase A (AURKA) is a member of the serine-threonine kinase family that regulates mitotic cell division from G_2 through to M phase of the cell cycle.[1] The *AURKA* gene maps to chromosome region 20q13.2. AURKA is expressed at low levels in normal cells, including dividing cells, and overexpression of AURKA has clear oncogenic potential.[2,3] Indeed, the *AURKA* gene is overexpressed in various types of cancer,[4] including leukemias.[5,6] Furthermore, correlations between the genetic dysregulation of *AURKA* and susceptibility to cancer, disease status, and prognosis have been described.[4] In particular, *AURKA* gene overexpression correlates with genetic instability and poor differentiation of cancer cells.[7,8] As AURKA expression is tightly regulated in normal tissues and overexpression correlates with malignant transformation, small molecular inhibitors have been developed that selectively target this protein in various tumors. A number of such molecules are currently in early phase clinical trials and preliminary data are encouraging.[9-12]

The overexpression of AURKA in cancer cells, but not in normal tissues, makes it an attractive target for tumor immunotherapy. We have previously shown that testis is the only tissue that expresses detectable levels of AURKA, which suggests that this antigen behaves like cancer/testis antigens.[13] Based on these findings, we previously studied the immunotherapeutic potential of AURKA and identified an HLA-A*0201-restricted antigenic nonamer epitope derived from the kinase domain (residues 207-215). The AURKA$_{207-215}$ epitope (YLILEYAPL) was recognized by CD8$^+$ cytotoxic T lymphocytes (CTLs) generated in vitro.[6] Furthermore, leukemic cells endogenously expressing AURKA were killed by these CTLs, indicating that the cognate epitope is naturally processed and presented in the context of HLA-A*0201 at levels sufficient for immunotherapeutic applications. In addition, Kobayashi and colleagues have identified HLA-class II–restricted AURKA-derived pentadecamer epitopes to which they could generate CD4$^+$ helper T cells that expressed antitumor reactivity.[14]

Immunotherapeutic interventions based on tumor antigen-specific *T-cell receptor* (*TCR*) gene transfer to redirect the specificity of other T cells has shown clinical success in patients with advanced melanoma.[15] However, this approach is complicated by several potential problems: (1) on-target adverse events directed against normal tissues, especially when affinity-enhanced TCRs are used[16]; (2) issues related to chain mispairing between the introduced and endogenous *TCR* α/β genes; and (3) off-target adverse events because of inherent cross-reactivity of the introduced TCR.[17] Although various solutions have been explored to minimize TCR chain mispairing, all current approaches have intrinsic limitations. To this end, we have recently developed a unique vector system that simultaneously delivers *siRNA*s, which specifically down-regulate endogenous *TCR* expression, and a *siRNA*-resistant relevant *TCR* construct (si-*TCR* vector).[18] Furthermore, the likelihood of adverse events related to expression of the introduced TCR may be minimized by the selection of tumor-specific antigens or cancer/testis antigens, rather than tumor-associated antigens. Indeed, a recent clinical study reported that redirected T-cell therapy using NY-ESO-1–specific *TCR* gene

Submitted June 11, 2011; accepted October 13, 2011. Prepublished online as *Blood* First Edition paper, October 24, 2011; DOI 10.1182/blood-2011-06-360354.

*K.N. and T.O. contributed equally to this work.

An Inside *Blood* analysis of this article appears at the front of this issue.

The online version of this article contains a data supplement.

The publication costs of this article were defrayed in part by page charge payment. Therefore, and solely to indicate this fact, this article is hereby marked "advertisement" in accordance with 18 USC section 1734.

transfer displayed antitumor efficacy against metastatic melanoma and metastatic synovial cell sarcoma without obvious toxicities mediated by the transferred T cells.[19]

In this study, we examined the antileukemic efficacy and safety of redirected T cells using HLA-A*0201–restricted $AURKA_{207-215}$–specific *TCR* gene transfer both in vitro and in vivo. The data demonstrate the feasibility of this approach for the treatment of human leukemias.

Methods

Cells and cell lines

Approval for this study was obtained from the Institutional Review Board of Ehime University Hospital (Protocol 0909001 and 0909002). Written informed consent was obtained from all patients, healthy volunteers, and parents of cord blood donors in accordance with the Declaration of Helsinki. B-lymphoblastoid cell lines (B-LCLs) were established by transformation of peripheral blood B-lymphocytes with Epstein-Barr virus. GANMO-1 (HLA-$A2^+$), MEG01 (HLA-$A2^-$), MEG01-A2 (*HLA-A*0201* gene-transduced MEG01), OUN-1 (HLA-$A2^-$), and KAZZ (HLA-$A2^-$) leukemia cell lines were cultured in RPMI 1640 with 10% FCS, antibiotics, and L-glutamine. The artificial antigen-presenting cell line C1R-A2 (HLA-$A*0201^+$) was a kind gift from Dr A. John Barrett (National Heart, Lung, and Blood Institute, Bethesda, MD). The Jurkat/MA cell line (kindly provided by Prof Erik Hooijberg, Vrije Universiteit Medisch Centrum, Amsterdam, The Netherlands) is a Jurkat cell subclone that lacks endogenous TCR expression and stably expresses both the human *CD8α* gene (*hCD8α*) and an *NFAT-luciferase* gene construct for the detection of signaling via newly introduced TCRs.[20] PBMCs and bone marrow mononuclear cells (BMMCs) from leukemia patients and healthy volunteers, and cord blood mononuclear cells (CBMCs) from healthy donors, were isolated by density gradient centrifugation and stored in liquid nitrogen until use. $CD34^+$ cells from CBMCs were isolated using $CD34^+$ cell-isolating immunomagnetic beads (Miltenyi Biotec).

Synthetic peptides and HLA-A*0201/peptide tetrameric complexes

The HLA-A*0201–restricted $AURKA_{207-215}$ nonameric peptide (YLILEYAPL) was purchased from Thermo Electron (Greiner Bio-One). Biotin-tagged soluble HLA-A*0201/AURKA monomers were produced as previously described.[21] Fluorochrome-labeled tetrameric complexes were generated by conjugation to streptavidin-PE (Prozyme) at a molar ratio of 4:1.[22] HLA-A*0201 tetramers were also produced with the HIV-1 p17 Gag-derived peptide epitope SL9 (SLYNTVATL, residues 77-85) for control purposes.

Generation of an $AURKA_{207-215}$-specific CTL clone

A novel $AURKA_{207-215}$-specific CTL clone designated AUR-2 was generated as previously described.[23] Briefly, monocyte-derived dendritic cells (Mo-DCs) were generated from $CD14^+$ PBMCs using 10 ng/mL recombinant human IL-4 and 75 ng/mL recombinant human GM-CSF (R&D systems), then matured with 100 U/mL recombinant human TNF-α (Dainippon Pharmaceutical). $CD8^+$ T cells (1×10^5) were stimulated with 10^4 autologous mature $AURKA_{207-215}$ peptide-loaded (10μM) Mo-DCs in a 96-well round-bottomed plate. One week later, the $CD8^+$ T cells were restimulated similarly, and 10 U/mL recombinant human IL-2 (Roche) was added after a further 4 days. Thereafter, $CD8^+$ T cells were restimulated weekly with 10^5 autologous $AURKA_{207-215}$ peptide-pulsed (10μM) PBMCs treated with mitomycin-C (MMC; Kyowa Hakko). Epitope-dependent target cell cytotoxicity was examined using standard ^{51}chromium (^{51}Cr)–release assays.

ELISPOT

ELISPOT assays were conducted as previously described.[22] Briefly, 96-well flat-bottomed MultiScreen-HA plates with a nitrocellulose base (Millipore) were coated overnight at 4°C with 10 μg/mL anti-IFN-γ monoclonal antibody (mAb; R&D Systems). After washing with PBS, cultured $CD8^+$ T cells were stimulated with 5×10^4 $AURKA_{207-215}$ peptide-pulsed (1μM) or unpulsed C1R-A2 cells/well for 20 hours at 37°C in a 5% CO_2 atmosphere. Subsequently, the wells were vigorously washed with PBS/0.05% tween 20 and incubated with polyclonal rabbit anti–IFN-γ Ab (Endogen) for 90 minutes at room temperature. The wells were then washed again and incubated for 90 minutes with peroxidase-conjugated goat anti–rabbit IgG Ab (Zymed). Spots were visualized by the addition of 100 μL substrate, comprising 0.1M sodium acetate buffer (pH 5.0) containing 3-amino-9-ethylcarbazole (Sigma-Aldrich) and 0.015% H_2O_2, for 40 minutes at room temperature and counted under a light microscope.

Cloning of full-length *TCR* α and β chain genes from the AUR-2 CTL clone and retroviral vector construction

Total RNA was extracted from the HLA-A*0201–restricted $AURKA_{207-215}$-specific CTL clone AUR-2 using the FastPure RNA Kit (Takara Bio) according to the manufacturer's instructions. Full-length *TCR* α and β genes were cloned as previously described.[24] Briefly, cDNA was amplified using a 5′-RACE primer and 3′-constant region primers as follows: (1) 5′-TCAGCTGGACCACAGCCGCAGCGT-3′ for TCR Cα; (2) 5′-TCAGAAATCCTTTCTCTTGAC-3′ for TCR Cβ1; and (3) 5′-CTAGCCTCTGGAATCCTTTCTCTT-3′ for TCR Cβ2. The conditions for PCR were: one cycle at 94°C for 3 minutes, followed by 30 cycles at 94°C for 40 seconds, 58°C for 40 seconds and 72°C for 1 minute, with a final extension phase at 72°C for 5 minutes. Each *TCR* α and β chain amplicon was cloned into the pMD20 TA cloning vector (Takara Bio), and sequenced using the BigDye Terminator v3.1 Cycle Sequencing Kit (Applied Biosystems) and an ABI 3730xl sequencer (Applied Biosystems). Full-length *TCR* α and β genes were then cloned into the bicistronic pMS3 retroviral vector, which is a pME1-5 derivative that contains the murine stem cell virus (MSCV) LTR (Takara Bio) in place of the 3′LTR (pMS3-*AURKA-TCR*, Figure 1). Ecotropic retrovirus particles were obtained by transient transfection of HEK293 T cells with the TCR construct and helper plasmids (pGP vector and pE-eco vector; Takara Bio). GaLV-pseudotyped retrovirus particles were obtained by consecutive transfection into PG13 cells. The pMS3-*AURKA-TCR* GaLV-pseudotyped retroviruses were used for AURKA-specific *TCR* α and β gene transduction.

Transduction of $AURKA_{207-215}$-specific *TCR genes*

Jurkat/MA cells and healthy donor T cells were genetically modified to express the AURKA-specific TCR using RetroNectin (Takara Bio) as previously described.[18] Briefly, 1×10^6 healthy donor T cells per well in GT-T503 (Takara Bio) with 5% human serum, 0.2% human albumin, 50 U/mL recombinant human IL-2 (R&D Systems), 5 ng/mL recombinant human IL-7 (R&D Systems), 10 ng/mL recombinant human IL-15 (PeproTech Inc), and 100 ng/mL recombinant human IL-21 (Shenandoah Biotechnology Inc) were added on day 1 to a 24-well culture plate pretreated with antihuman CD3 mAb (BioLegend). Jurkat/MA cells were cultured in IMDM with 8% FCS and 50 μg/mL hygromycin B (Invitrogen). On day 3, cultured T cells or Jurkat/MA cells were transferred on to a retrovirus-preloaded RetroNectin-coated 24-well plate, centrifuged at 2000*g* for 2 hours and rinsed with PBS. Cells were then applied to the retrovirus-preloaded RetroNectin-coated 24-well plate again for the second transduction. AURKA-specific *TCR*-transduced T cells were stimulated weekly with MMC-treated C1R-A2 cells loaded with $AURKA_{207-215}$ peptide (1μM) for further functional experiments.

Flow cytometric analysis

The AUR-2 CTL clone expresses the *TRBV10-3* gene, denoted in IMGT nomenclature.[25] This corresponds to TCR Vβ12 in the Arden nomenclature.[26] Accordingly, anti-TCR Vβ12 mAb was used to detect $AURKA_{207-215}$-specific *TCR*-transduced cells. After 4 to 6 days, transduced cells were analyzed by flow cytometry using anti-TCR Vβ12-FITC (Beckman Coulter), anti-CD8–FITC (BD Biosciences) or anti-CD8–PE (BioLegend), and HLA-A*0201/$AURKA_{207-215}$ tetramer-PE (only with anti-CD8–FITC).

Intracellular expression of Foxp3 and $AURKA_{207-215}$–responsive IFN-γ production by $AURKA_{207-215}$–specific *TCR*-transduced $CD4^+$ T cells were analyzed using anti–Foxp3-PE (e-Bioscience) and anti–IFN-γ–FITC (BD Biosciences). Data were acquired using a FACS Calibur flow cytometer and analyzed with either Cell Quest (BD Biosciences) or FlowJo Version 7.2.2 software (TreeStar Inc).

CFSE dilution assay

To measure epitope-responsive proliferation of $AURKA_{207-215}$–specific *TCR*-transduced $CD8^+$ T cells in the presence or absence of similarly redirected $CD4^+$ T cells, $CD8^+$ T cells were labeled with CFSE (Molecular Probe Inc) as described previously.[27] After 3 days, CFSE dilution within the $CD8^+$ T-cell population was assessed by flow cytometry.

Epitope-responsive luciferase production by $AURKA_{207-215}$–specific *TCR*-transduced Jurkat/MA cells

To verify the functionality of the cloned $AURKA_{207-215}$–specific *TCR* α and β chains, we used the TCR^- Jurkat/MA cell line, which stably expresses *hCD8α* and an *NFAT-luciferase* reporter gene (Jurkat/MA/CD8α/luc), as follows. pMS3-*AURKA-TCR* was retrovirally transduced into Jurkat/MA/CD8α/luc cells. Cells expressing TCR Vβ12 were isolated for functional analysis. Briefly, HLA-A*0201$^+$ B-LCL cells were loaded with titrated doses of $AURKA_{207-215}$ peptide or the irrelevant SL9 peptide (10μM; HIV-1 p17 Gag, residues 77-85) and used to stimulate 8×10^5 *TCR* gene-modified Jurkat/MA/CD8α/luc cells (effector:target ratio 2:1) for 12 hours. The cells were then lysed and subjected to luciferase assay using the PicaGene-Dual-SeaPansy Kit (TOYOinki) according to manufacturer's instructions. Luciferase activity was measured using a Lumicounter700 (MicrotecNition).

IFN-γ secretion assay

$AURKA_{207-215}$–specific *TCR*-transduced $CD4^+$ or $CD8^+$ T cells (5×10^5) were incubated with 10^5 $AURKA_{207-215}$ peptide-pulsed (1μM) or unpulsed C1R-A2 cells for 24 hours. For the inhibition assay, cells were cultured in the presence of either an anti-HLA class I framework mAb (w6/32; ATCC) or a control anti–HLA-DR mAb (L243; ATCC). Cytokine production patterns were assessed using a bead-based immunoassay kit (Becton Dickinson). IFN-γ in the culture supernatant was measured using an ELISA kit (Pierce) according to the manufacturer's instructions. Streptavidin-HRP was used for color development, and luminointensity was measured using IMMUNO-MINI (NJ-2300; Microtec).

Cytotoxicity assay

Standard ^{51}Cr release assays were performed as previously described.[28] Briefly, 10^4 unpulsed or peptide-pulsed target cells were labeled with ^{51}Cr ($Na_2{}^{51}CrO_4$; MP Bio Japan) and incubated at various ratios with effector cells in 200 μL of culture medium in 96-well round-bottomed plates. To assess HLA class I restriction, target cells were incubated with 10 μg/mL w6/32 mAb or the control L243 mAb for 1 hour, then incubated with effector cells for 5 hours. After incubation, 100 μL supernatant was collected from each well to measure ^{51}Cr release. The percentage specific lysis was calculated as: (experimental release cpm − spontaneous release cpm)/(maximal release cpm − spontaneous release cpm) × 100 (%).

Quantitative analysis of *AURKA* mRNA expression

Quantitative real-time PCR (qRT-PCR) for *AURKA* mRNA was performed as described previously.[6] Briefly, total RNA was extracted using an RNeasy Mini Kit (QIAGEN) and cDNA was synthesized. qRT-PCRs for *AURKA* mRNA (Hs00269212_ml) and glyceraldehyde-3-phosphate dehydrogenase (*GAPDH*) mRNA (4326317E) as an internal control were performed using the TaqMan Gene Expression assay (Applied Biosystems) in accordance with the manufacturer's instructions and an ABI Prism 7700 Sequence Detection System (Applied Biosystems). The expression level of *AURKA* mRNA was corrected by reference to that of *GAPDH* mRNA, and the relative amount of *AURKA* mRNA in each sample was calculated by the comparative ΔCt method.

AURKA protein expression analysis by Western blotting

For the analysis of protein expression, Western blotting was performed as described previously.[6] Briefly, cell lysates were subjected to 10% SDS-PAGE (e-PAGEL, ATTO) and blotted onto PVDF membranes (Bio-Rad Laboratories). The blots were incubated first with anti-AURKA mouse mAb (Abcam), then with HRP-conjugated anti–mouse IgG (GE Healthcare). The probed proteins were visualized using an enhanced chemiluminescence system (GE Healthcare). Subsequently, the blotted membranes were stripped and reprobed with anti–β-actin mouse mAb (Sigma-Aldrich) to confirm equivalent protein loading between samples.

Antileukemia effect of $AURKA_{207-215}$–specific *TCR*-transduced T cells in xenograft mouse models

All in vivo experiments were approved by the Ehime University animal care committee. For the Winn assay, 5×10^6 GANMO-1 cells and 2.5×10^7 $AURKA_{207-215}$–specific *TCR* gene-transduced or non–gene-modified $CD8^+$ T cells were inoculated per mouse (n = 4 per group). The cells were suspended in 300 μL PBS and injected subcutaneously into the left flank of NOG mice (Non-Obese Diabetic/Severe Combined Immuno-Deficiency/IL-2 receptor γ-chain allelic mutation; *NOD*/Shi-*scid*/IL-2R γ^{null})[29] aged 5-6 weeks (Central Institute for Experimental Animals). Mice were subsequently injected intravenously with either 5×10^6 $AURKA_{207-215}$–specific *TCR* gene-modified cells, AUR-2 cells or unmodified $CD8^+$ T cells, as per the initial inoculation, on a weekly basis for a total of 5 infusions. Tumor size was measured every 5 days until the mice died or were euthanized because of tumor progression.

For adoptive transfer experiments, NOG mice aged 9 weeks were similarly inoculated with 5×10^6 of GANMO-1 cells. Intravenous administration of either 5×10^6 $AURKA_{207-215}$–specific *TCR* gene-transduced or non–gene-modified $CD8^+$ T cells commenced on the same day (day 0), and was continued on a weekly basis thereafter until the mice died or were euthanized because of tumor progression.

Statistical analysis

The paired *t* test was used to assess differences between groups; a P value $< .05$ was considered significant.

Results

Generation of a novel HLA-A*0201–restricted $AURKA_{207-215}$–specific CTL clone (AUR-2) and retroviral expression of the full-length *TCR* α and β genes

Characteristics of the newly established HLA-A*0201-restricted $AURKA_{207-215}$–specific CTL clone (AUR-2) are shown in Figure 1. AUR-2 was stained uniformly with the HLA-A*0201/$AURKA_{207-215}$ tetramer, but not with the irrelevant HLA-A*0201/Gag_{77-85} tetramer (Figure 1A). In cytotoxicity assays, AUR-2 displayed moderate levels of functional sensitivity in response to cognate peptide (Figure 1B). Epitope-dependent production of IFN-γ was confirmed in ELISPOT assays (Figure 1C). Peptide specificity and HLA restriction were further demonstrated in cytotoxicity assays with different target cells (Figure 1D). In addition, AUR-2 lysed the HLA-A*0201$^+$ leukemia cell line GANMO-1, which overexpresses *AURKA* mRNA, but not the HLA-A*0201$^-$ negative cell lines MEG01 and K562, both of which also express *AURKA* mRNA at high levels (Figure 1E). The rearranged *TCR* α and β genes of AUR-2 were sequenced and found to comprise the germ line gene segments *TRAV3/TRAJ20/TRAC* and *TRBV10-3/TRBJ1-1/TRBC1*, respectively; both full-length genes were cloned into a novel bicistronic retroviral vector (Figure 1F).

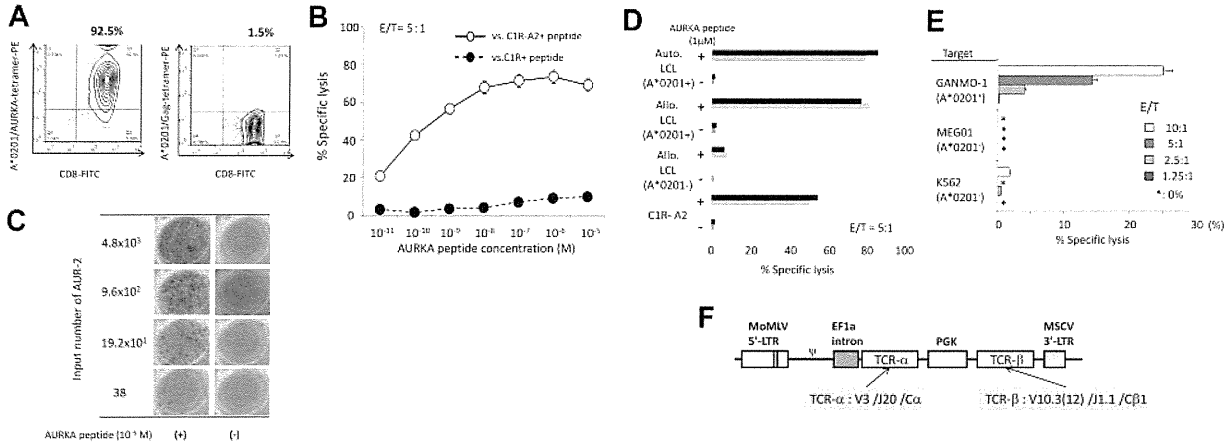

Figure 1. Characteristics of the AURKA$_{207-215}$–specific CTL clone AUR-2. (A) Representative flow cytometry plots showing staining of AUR-2 with the HLA-A*0201/AURKA$_{207-215}$ tetramer (left) and the irrelevant HLA-A*0201/Gag$_{77-85}$ tetramer (negative control; right). (B) The cytotoxic activity of AUR-2 was measured in ^{51}Cr-release assays against C1R-A2 or C1R (negative control) cells loaded with a range of AURKA$_{207-215}$ peptide concentrations as indicated. E/T indicates effector:target ratio. (C) IFN-γ ELISPOT assays were conducted using C1R-A2 target cells loaded with 1 μM AURKA$_{207-215}$ peptide and AUR-2 CTL at different input numbers as shown. (D) ^{51}Cr-release assays were conducted using AUR-2 CTL with unpulsed or AURKA$_{207-215}$ peptide-pulsed (1 μM) HLA-A*0201$^+$ autologous or allogeneic B-LCLs, C1R-A2 cells or HLA-A*0201$^-$ allogeneic B-LCLs as indicated. E/T indicates effector:target ratio. (E) The cytotoxic activity of AUR-2 CTL against the indicated leukemia cell lines was measured in ^{51}Cr-release assays. GANMO-1, HLA-A*0201$^+$; MEG01 and K562, HLA-A*0201$^-$. Expression of *AURKA* mRNA and AURKA protein in these leukemia cell lines is shown in supplemental Figure 2. E/T indicates effector:target ratio. (F) Construction of a novel retroviral vector encoding full-length AURKA–specific *TCR* α and β genes derived from AUR-2. MoMLV indicates Moloney murine leukemia virus; LTR, long terminal repeat; EF1a, elongation factor 1a; PGK, phosphoglycerate kinase promoter; and MSCV, murine stem cell virus. Error bars represent SDs.

Functional reconstitution of the AURKA$_{207-215}$–specific TCR heterodimer in Jurkat/MA cells

To validate the functionality of the cloned *TCR* genes, both chains were expressed in the TCR$^-$ cell line Jurkat/MA/CD8α/luc, which contains a luciferase reporter gene to monitor TCR signaling (Figure 2A). AUR-2*TCR*–transduced, Vβ12-selected Jurkat/MA/CD8α/luc cells (Figure 2B) were incubated with C1R-A2 cells pulsed with a range of AURKA$_{207-215}$ peptide concentrations, then assayed for luciferase activity. The *TCR* gene-modified Jurkat/MA/CD8α/luc cells produced luciferase in response to stimulation with AURKA$_{207-215}$ peptide-loaded C1R-A2 cells in a dose-dependent manner (Figure 2C). Compared with the parental AUR-2 CTL clone (Figure 1B), the *TCR*-transduced Jurkat/MA cells displayed low levels of peptide sensitivity. To address this functional discrepancy, we assessed cell-surface expression of TCR α/β, CD3, CD8α, CD11a, and CD28 (supplemental Figure 1, available on the *Blood* Web site; see the Supplemental Materials link at the top of the online article). The *TCR*-transduced Jurkat/MA cells expressed lower surface levels of TCR α/β, CD3 and CD8α compared with both similarly activated normal CD8$^+$ T cells and the parental AUR-2 CTL clone. Furthermore, CD11a and CD28 were almost absent from the transfectant cells. These findings may explain the observed differences in functional sensitivity between AUR-2 *TCR*-transduced Jurkat/MA cells and the parental CTL clone.

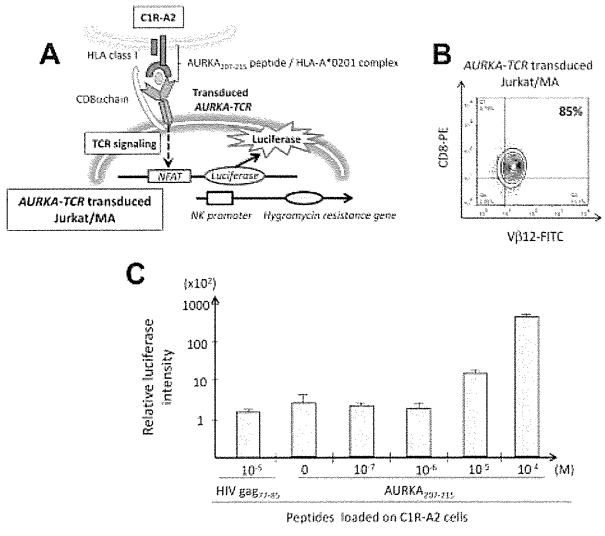

Figure 2. Functional retroviral expression of the AURKA$_{207-215}$–specific TCR. (A) Schematic representation of the luciferase assay using AURKA$_{207-215}$–specific *TCR*-transduced Jurkat/MA cells. NFAT indicates nuclear factor activated T cells; and NK, natural killer. (B) AURKA$_{207-215}$–specific *TCR*-transduced Jurkat/MA cells express Vβ12 but label poorly with cognate tetramer (data not shown), probably because of the low levels of surface CD8α expression. (C) AURKA$_{207-215}$–specific *TCR*-transduced Jurkat/MA cells were stimulated with peptide-pulsed C1R-A2 cells as shown and subjected to luciferase assay. Error bars represent SDs.

AURKA$_{207-215}$–specific *TCR* gene-transduced CD8$^+$ T cells exert antileukemia reactivity in vitro

Next, the AURKA$_{207-215}$–specific *TCR* was retrovirally introduced into normal CD8$^+$ T cells. Transduction efficiency determined by Vβ12 staining of *TCR* gene-modified T cells was 50%-70% (data not shown), and 20%-25% of the Vβ12$^+$ cells stained with the HLA-A*0201/AURKA$_{207-215}$ tetramer (Figure 3A). Isolated Vβ12$^+$ AURKA$_{207-215}$–specific *TCR* gene-transduced CD8$^+$ T cells displayed similar antigen sensitivity to the parental AUR-2 CTL clone (Figure 3B-C). Notably, however, the AURKA$_{207-215}$–specific *TCR* transductants produced higher quantities of IFN-γ in response to the same peptide-pulsed C1R-A2 targets (Figure 3C). On the basis of these observations, further experiments were carried out using these AURKA$_{207-215}$–specific *TCR* gene transfectants.

AURKA$_{207-215}$–specific *TCR*-transduced CD8$^+$ T cells displayed HLA class I–restricted, peptide-dependent IFN-γ production (Figure 3D), and target epitope–specific cytotoxic activity (Figure 3E). Furthermore, these redirected CD8$^+$ T cells selectively lysed the HLA-A*0201$^+$ leukemia cell line GANMO-1, which overexpresses AURKA, but not the HLA-A*0201$^-$ leukemia cell lines, MEG01, KAZZ, and OUN-1, which also overexpress AURKA (Figure 4A, supplemental Figure 2). In contrast,

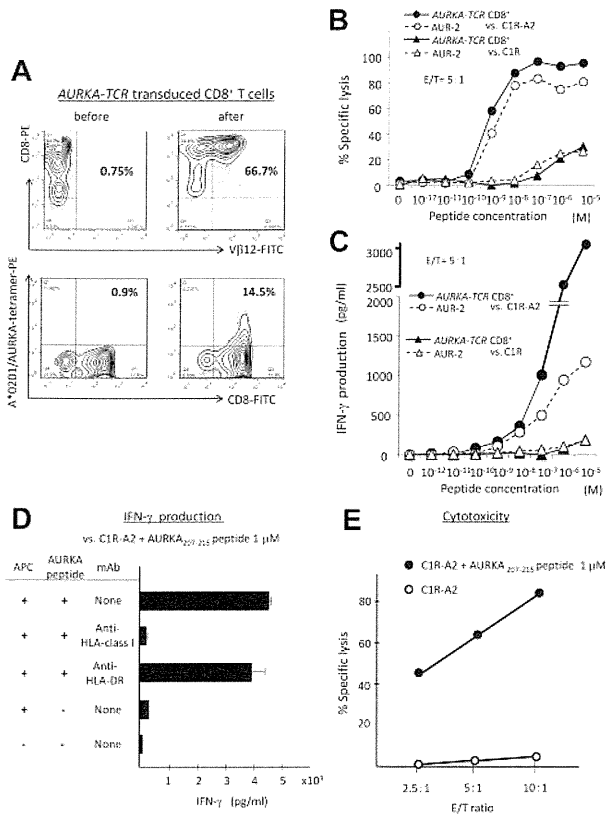

Figure 3. AURKA$_{207-215}$–specific *TCR*-transduced CD8$^+$ T cells display epitope-specific functionality. (A) Representative flow cytometry plots showing staining of AURKA$_{207-215}$–specific *TCR*-transduced CD8$^+$ T cells with anti-TCR Vβ12 mAb and HLA-A*0201/AURKA$_{207-215}$ tetramer. (B) The same AURKA$_{207-215}$ *TCR*-transduced CD8$^+$ T cells shown in panel A were tested in ^{51}Cr-release assays against C1R (negative control) and C1R-A2 cells pulsed with the indicated concentrations of AURKA$_{207-215}$ peptide. The parental AUR-2 CTL clone was tested in parallel. E/T indicates effector:target ratio. (C) IFN-γ production by AURKA$_{207-215}$–specific *TCR*-transduced CD8$^+$ T cells was measured in a similar format to that described for panel B. (D) Effects of HLA class I and class II blockade on the production of IFN-γ by AURKA$_{207-215}$–specific *TCR*-transduced CD8$^+$ T cells stimulated with cognate peptide-loaded (1 μM) C1R-A2 cells. (E) Cytotoxic activity of AURKA$_{207-215}$–specific *TCR*-transduced CD8$^+$ T cells against unpulsed or cognate peptide-loaded (1 μM) C1R-A2 cells as a function of effector:target (E/T) ratio. Error bars represent SDs.

HLA-A*0201$^+$ PBMCs (n = 3), PHA-stimulated lymphoblasts representing highly mitotic normal cells (n = 3), and normal cord blood CD34$^+$ cells (CB-CD34$^+$cells; n = 2) were not lysed by these AURKA$_{207-215}$–specific *TCR* transductants (Figure 4B). *AURKA* mRNA expression relative to K562 for each group (mean ± SD) was 0.02 ± 0.008 for PBMCs, 0.25 ± 0.005 for PHA-lymphoblasts and 0.21 ± 0.09 for CB-CD34$^+$ cells, which indicated relatively low expression levels of *AURKA* mRNA among these cells compared with K562. The cytotoxic activity of AURKA$_{207-215}$–specific *TCR*-transduced CD8$^+$ T cells against GANMO-1 and cognate peptide-loaded B-LCLs was significantly diminished by an anti-HLA class-I mAb but not by an anti–HLA-DR mAb (Figure 4C-D). To confirm recognition of the endogenously processed AURKA$_{207-215}$ epitope in the context of HLA-A*0201 expressed by leukemia cells, we retrovirally transduced the *HLA-A*0201* gene into MEG01 cells (MEG01-A2; Figure 4E). Parental MEG01 cells do not express HLA-A*0201, but abundantly overexpress both *AURKA* mRNA and AURKA protein (supplemental Figure 2). Compared with MEG01, MEG01-A2 were susceptible to the cytotoxic effects of AURKA$_{207-215}$–specific *TCR*-transduced CD8$^+$ T cells (Figure 4F). Collectively, these data indicate that the antileukemia reactivity mediated by AURKA$_{207-215}$–specific *TCR*-transduced CD8$^+$ T cells occurs through the recognition of endogenously processed and presented AURKA$_{207-215}$ peptide in the context of HLA-A*0201 on the surface of leukemia cells.

Next, the antileukemia reactivity mediated by these redirected AURKA$_{207-215}$–specific CD8$^+$ T cells was tested against freshly isolated leukemia cells in vitro (Figure 5). *AURKA* mRNA was overexpressed in all 6 leukemia samples as determined by qRT-PCR. Leukemia cells isolated from HLA-A*0201$^+$ patients (1-3), but not HLA-A*0201$^-$ patients (4-6) were lysed by the AURKA$_{207-215}$–specific *TCR*-transduced CD8$^+$ T cells. Thus, our data show that the AUR-2 TCR confers AURKA$_{207-215}$ specificity to donor CD8$^+$ T cells transduced with both TCR chains, and that normal cells, including actively cycling cells and hematopoietic progenitor cells, are not lysed by these redirected T cells.

AURKA$_{207-215}$–specific *TCR*-transduced CD4$^+$ T cells respond to cognate antigen

Next, we examined antigen reactivity in isolated populations of Vβ12$^+$ AURKA$_{207-215}$–specific *TCR*-transduced CD4$^+$ T cells (Figure 6A). AURKA$_{207-215}$–specific *TCR*-transduced CD4$^+$ T cells successfully produced IFN-γ in response to stimulation with AURKA$_{207-215}$ peptide-loaded C1R-A2 cells; this response was substantially reduced by HLA class I blockade, and a partial response reduction was also observed with HLA class II blockade (Figure 6B). These redirected CD4$^+$ T cells did not express Foxp3, which is a key molecular signature of regulatory T cells (supplemental Figure 3A), and the cognate antigen-specific proliferative response of AURKA$_{207-215}$–specific *TCR*-transduced CD8$^+$ T cells was actually enhanced in the presence of redirected CD4$^+$ T cells but not in the presence of non–gene-modified CD4$^+$ T cells (supplemental Figure 3B). Furthermore, AURKA$_{207-215}$–specific *TCR*-transduced CD4$^+$ T cells produced significant amounts of IL-2, TNF-α, and IFN-γ, but not IL-4 or IL-10 (supplemental Figure 4).

These observations suggest that AURKA$_{207-215}$–specific *TCR*-transduced CD4$^+$ T cells might be able to function as epitope-specific Th1 helper T cells, and that the interaction between T cell–expressed CD4 and target cell-expressed HLA class II molecules facilitates HLA class I–restricted AURKA$_{207-215}$–specific IFN-γ production.

AURKA$_{207-215}$–specific *TCR*-transduced CD8$^+$ T cells exhibit antileukemia reactivity in vivo

The in vivo antileukemia reactivity of AURKA$_{207-215}$–specific *TCR*-transduced CD8$^+$ T cells was assessed using the Winn assay and a therapeutic adoptive transfer model.

In the Winn assay, NOG mice were initially coinjected with GANMO-1 cells (5×10^6) and either 2.5×10^7 AURKA$_{207-215}$-specific *TCR* gene-modified or non–gene-modified CD8$^+$ T cells; 5 weekly infusions of the respective CD8$^+$ T-cell populations (5×10^6 cells per infusion) were subsequently administered. Treatment with AURKA$_{207-215}$–specific *TCR*-transduced CD8$^+$ T cells completely prohibited the engraftment and growth of inoculated leukemia cells for more than 2 months (Figure 7A), and significantly prolonged survival (Figure 7B). Similar results were obtained with AUR-2 cells in a parallel regimen (supplemental Figure 5). In contrast, non–gene-modified CD8$^+$ T cells did not prohibit leukemia growth. In a therapeutic adoptive transfer model, intravenously injected AURKA$_{207-215}$–specific *TCR*-transduced

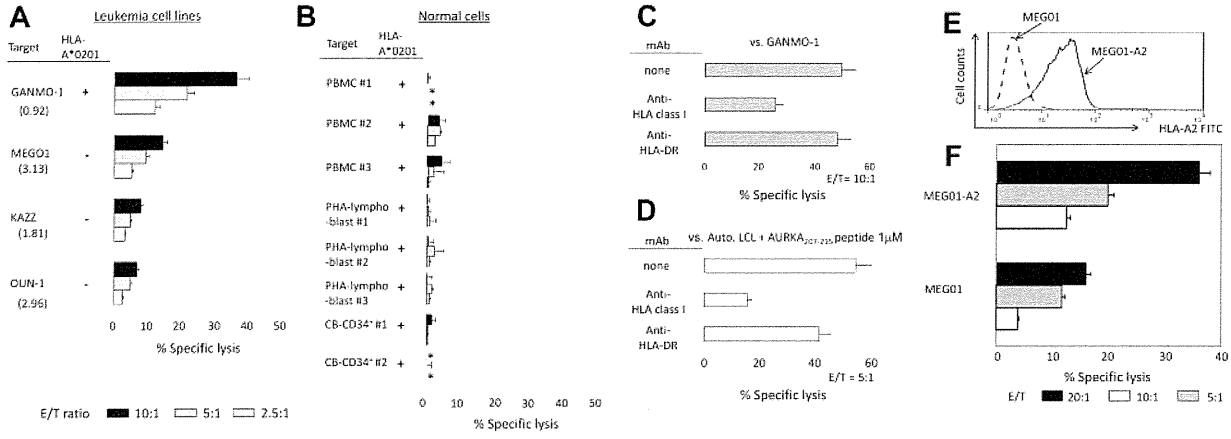

Figure 4. AURKA$_{207-215}$–specific *TCR*-transduced CD8$^+$ T cells can distinguish leukemia cells from normal cells on the basis of AURKA expression levels. (A) AURKA$_{207-215}$–specific *TCR*-transduced CD8$^+$ T cells exhibit antileukemia reactivity in an HLA-A*0201-dependent fashion. The HLA-A*0201$^+$ leukemia cell line GANMO-1 was lysed by AURKA$_{207-215}$–specific *TCR*-transduced CD8$^+$ T cells as a function of effector:target (E/T) ratio; no significant lysis was observed with the HLA-A*0201$^-$ leukemia cells lines MEG01, KAZZ and OUN-1. All of the tested leukemia cell lines overexpress *AURKA* mRNA; numbers in parentheses indicate *AURKA* mRNA expression relative to K562, and correlations with AURKA protein expression are shown in supplemental Figure 2. (B) The same AURKA$_{207-215}$–specific *TCR*-transduced CD8$^+$ T cells used in panel A at the same E/T ratios were tested in ^{51}Cr-release assays for potentially damaging effects against normal cells. No significant lysis was observed with HLA-A*0201$^+$ PBMCs (n = 3), PHA-lymphoblasts representing normal mitotic cells (n = 3) or normal cord blood–derived CD34$^+$ cells (CB-CD34$^+$) encompassing normal hematopoietic progenitor cells (n = 2). *AURKA* mRNA expression relative to K562 was 0.02 ± 0.008 for PBMCs, 0.25 ± 0.005 for PHA-lymphoblasts and 0.21 ± 0.09 for CB-CD34$^+$ cells (* indicates less than detectable). (C) Effects of HLA class I and class II blockade on the cytotoxic activity of AURKA$_{207-215}$–specific *TCR*-transduced CD8$^+$ T cells against GANMO-1 leukemia cells. E/T, effector:target ratio. (D) As for panel C, showing the effects of HLA class I and class II blockade on the lysis of autologous B-LCLs loaded with AURKA$_{207-215}$ peptide (1 μM). (E) Flow cytometric confirmation of HLA-A*0201 expression by MEG01-A2 cells. (F) Enhanced lysis of MEG01-A2 cells relative to parental MEG01 cells by AURKA$_{207-215}$–specific *TCR*-transduced CD8$^+$ T cells confirms recognition of endogenously processed AURKA$_{207-215}$ peptide presented in the context of HLA-A*0201. E/T indicates effector:target ratio. Error bars represent SDs.

CD8$^+$ T cells, but not non–gene-modified CD8$^+$ T cells, significantly suppressed the growth of inoculated leukemia cells in vivo ($P < .02$; Figure 7C). Statistically significant tumor suppression was achieved on day 65, after 10 adoptive infusions. Thereafter, all mice (n = 4) treated with non–gene-modified CD8$^+$ T cells died by day 85. 2 mice treated with AURKA$_{207-215}$–specific *TCR*-transduced CD8$^+$ T cells died from other causes (1 on day 45 and 1 on day 70); the other 2 mice in this group survived longer than 90 days and were finally euthanized because of disease progression. Collectively, these observations indicate that AURKA$_{207-215}$–specific *TCR*-transduced CD8$^+$ T cells exhibit antileukemia reactivity in vivo.

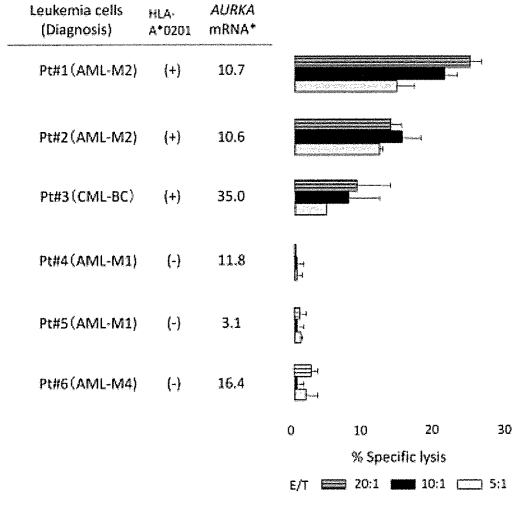

Figure 5. AURKA$_{207-215}$–specific *TCR*-transduced CD8$^+$ T cells kill freshly isolated leukemia cells in vitro. Freshly isolated HLA-A*0201$^+$ (n = 3) or HLA-A*0201$^-$ (n = 3) acute or chronic myeloid leukemia cells overexpressing *AURKA* mRNA were used as targets in ^{51}Cr-release assays with AURKA$_{207-215}$–specific *TCR*-transduced CD8$^+$ T cells at the indicated effector:target (E/T) ratios. AML, acute myeloid leukemia; BC, blast crisis; CML, chronic myeloid leukemia. M1, M2, and M4 refer to French-American-British classification subtypes (* indicates the expression of *AURKA* mRNA relative to the mean expression levels across 5 PBMC samples from healthy donors was determined by qRT-PCR and calculated using the comparative ΔCt method). Error bars represent SDs.

Discussion

In the setting of hematologic malignancies, *TCR* gene therapy targeting WT1 in leukemia,[30] and *chimeric antigen receptor* (*CAR*) gene therapy targeting CD33 in myeloid leukemias[31] and CD19, CD20, CD22, CD30, and the receptor tyrosine kinase-like orphan receptor 1 (ROR1) in B-cell malignancies,[32-38] are currently being investigated in preclinical studies or in early phase clinical trials.

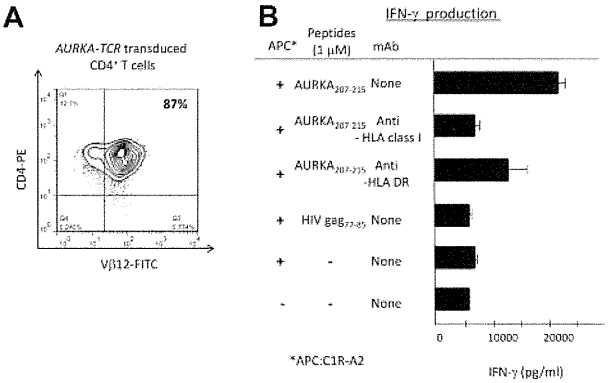

Figure 6. AURKA$_{207-215}$–*TCR* transduced CD4$^+$ T cells display antigen-specific Th1 cytokine production. (A) A representative flow cytometry plot showing surface Vβ12 expression by AURKA$_{207-215}$–specific *TCR*-transduced CD4$^+$ T cells. (B) *AURKA*$_{207-215}$–*TCR* transduced CD4$^+$ T cells produce IFN-γ in response to cognate peptide-loaded (1 μM) C1R-A2 cells; unpulsed or irrelevant (HIV p17 Gag SL9) peptide-pulsed C1R-A2 cells were used as negative controls. Cognate antigen-specific IFN-γ production was reduced to background levels in the presence of anti-HLA class I blocking mAb and inhibited in the presence of anti-HLA class II blocking mAb. APC, antigen-presenting cell. Error bars represent SDs.

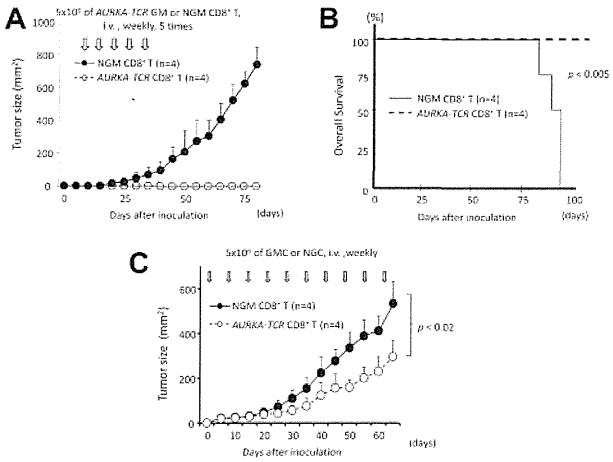

Figure 7. AURKA$_{207-215}$–specific *TCR*-transduced CD8$^+$ T cells mediate antileukemia reactivity in vivo. (A) Winn assay: tumor suppression curve. NOG mice were coinjected with GANMO-1 cells (5×10^6) and either 2.5×10^7 AURKA$_{207-215}$–specific *TCR* gene-modified (*AURKA-TCR*) or non–gene-modified (NGM) CD8$^+$ T cells (n = 4 group). Subsequently, 5 weekly infusions of the respective CD8$^+$ T-cell populations (5×10^6 cells per infusion) were administered intravenously. Tumor growth was monitored every 5 days. (B) Winn assay: survival curve. Treatment with AURKA$_{207-215}$–specific *TCR* gene-modified (*AURKA-TCR*) CD8$^+$ T cells significantly prolonged survival ($P < .005$). (C) Therapeutic adoptive transfer model. NOG mice (n = 4 per group) were inoculated with 5×10^6 of GANMO-1 cells. Intravenous administration of either 5×10^6 AURKA$_{207-215}$–specific *TCR* gene-modified (*AURKA-TCR*) or non–gene-modified (NGM) CD8$^+$ T cells commenced on the same day and was continued weekly thereafter. Therapeutic infusions of AURKA$_{207-215}$–specific *TCR* gene-modified CD8$^+$ T cells significantly suppressed tumor growth ($P < .02$). Error bars represent SDs.

Although adoptive antileukemia/lymphoma therapy with redirected T cells using tumor antigen-specific *TCR* or *CAR* gene transfer remains in its infancy, emerging evidence supports the development of such therapeutic options.

A number of preclinical and clinical studies of tumor antigen-specific *TCR* gene therapy have underscored the fact that appropriate antigen selection is essential to minimize the likelihood of on-target adverse events mediated by redirected T cell recognition of normal tissues expressing self-derived specificities.[39] This concept is further supported by a recent study of NY-ESO-1–specific *TCR* gene transfer.[19] In this report, objective clinical responses were observed in 5 of 11 patients with metastatic melanoma and 4 of 6 patients with metastatic synovial cell sarcoma without any toxicity related to engineered T cell activity.[19] Thus, the exploration of novel tumor antigens to identify safe and effective targets for *TCR* gene therapy is warranted, especially in the context of hematologic malignancies.

Previously, we reported a significant correlation between the overexpression of *AURKA* mRNA and the aggressiveness of lymphoma cells.[13] Furthermore, we found that *AURKA* mRNA is overexpressed in a large proportion of freshly isolated human leukemia cells.[6] However, in normal tissues, *AURKA* mRNA expression is largely limited to the testis.[13] Subsequently, we identified an immunogenic nonamer epitope derived from AURKA that was presented in the context of HLA-A*0201.[6] In the present study, we set out to examine the feasibility of redirected T cell–based adoptive immunotherapy for the treatment of human leukemia using a TCR derived from an HLA-A*0201–restricted AURKA$_{207-215}$–specific CD8$^+$ T-cell clone (AUR-2). Expression of this TCR in CD8$^+$ T cells conferred antileukemia reactivity both in vitro and in a xenogeneic mouse model of human leukemias. Furthermore, CD4$^+$ T cells could be redirected using this TCR to recognize the same HLA-A*0201–restricted AURKA$_{207-215}$ epitope. This represents a potentially important advantage, as the same TCR could redirect both helper (CD4$^+$) and cytotoxic (CD8$^+$) functions within the transduced T-cell population, which might sustain the antileukemia response in vivo after adoptive transfer.

Redirected CD8$^+$ T cells expressing the *TCR* cloned from AUR-2 displayed similar levels of functional sensitivity to the parental CTL clone. In vitro, AURKA$_{207-215}$–specific *TCR* gene-transduced CD8$^+$ T cells were able to lyse HLA-A*0201$^+$ human leukemia line GANMO-1 cells, which overexpress *AURKA* mRNA, and freshly isolated leukemia cells from HLA-A*0201$^+$ patients. This antileukemia reactivity was implemented through recognition of the endogenously processed AURKA$_{207-215}$ epitope presented in the context of HLA-A*0201. Importantly, these AURKA$_{207-215}$-specific *TCR*-transduced CD8$^+$ T cells did not lyse HLA-A*0201$^+$ normal PBMCs, mitotic PHA-lymphoblasts or cord blood CD34$^+$ cells; these data suggest that on-target adverse effects would be minimal in clinical applications. Furthermore, we demonstrated the efficacy of AURKA$_{207-215}$–specific *TCR*-transduced CD8$^+$ T cells in vivo by showing the inhibition of leukemia cell growth in a xenograft mouse model. As many hematopoietic progenitor cells actively proliferate and will therefore have enhanced AURKA expression levels, these cells may become targets for AURKA$_{207-215}$–specific *TCR*-transduced CD8$^+$ T cells in vivo, as is the case with selective AURKA inhibitors.[40] However, our observations suggest that redirected CD8$^+$ T cells targeting AURKA may not cause severe bone marrow failure, although further studies are needed to substantiate this point.

Notably, AURKA is overexpressed in the fraction of bone marrow cells that encompasses myeloid leukemia stem cells.[6,41] Recently, targeting leukemia stem cells has been highlighted as a treatment strategy to prevent disease progression in a durable fashion.[42] Monoclonal antibodies that target leukemia stem cell surface antigens have been proposed for this purpose. Examples of such molecules include CD123 (IL3Rα)[43] and TIM-3.[44] Cellular immunotherapy targeting antigens that are preferentially overexpressed in leukemia stem cells has also been proposed. In this regard, WT1 appears to be a particularly attractive candidate.[45] Indeed, we have cloned an HLA-A*2402–restricted WT1$_{235-243}$–specific *TCR* gene into our unique si-*TCR* vector to address the potential of this approach.[46] With respect to AURKA, we previously described that the CD34$^+$CD38$^-$ fraction of bone marrow mononuclear cells from CML patients expressed high levels of *AURKA* mRNA and that these cells were susceptible to AURKA-specific CTL-mediated lysis.[6] Thus, redirected T cell–based immunotherapy targeting AURKA might be able to suppress leukemia stem cells. Furthermore, such an approach may be synergistic with the administration of selective AURKA inhibitors, for example in the treatment of relapsed leukemia after allogeneic hematopoietic stem cell transplantation.

Strategic options to achieve better clinical responses in the field of *TCR* gene transfer are much needed. The manipulation of helper CD4$^+$ T cells is one such approach.[24,47,48] To date, the adoptive transfer of redirected CD4$^+$ T cells concurrently with CD8$^+$ T cells expressing the same tumor-specific TCR gene has not been described; however, this is an intriguing notion that could enhance the antitumor reactivity of such adoptive transfer approaches in vivo. In recognition of this possibility, we found that AURKA$_{207-215}$ *TCR*-transduced CD4$^+$ T cells displayed Th1 cytokine production in response to the HLA-A*0201/AURKA$_{207-215}$ epitope in vitro. The effects of such activity in vivo, however, remain to be clarified. Another approach to combined immunotherapy employs peptide vaccination. Indeed, vaccination with the relevant peptide has been

shown to enhance the antitumor functionality of infused gene-modified T cells.[49] The feasibility of this combination strategy using $AURKA_{207-215}$ peptide vaccination is currently under investigation.

In summary, we have demonstrated the feasibility of antileukemia adoptive therapy using AURKA-specific *TCR* gene transfer. As AURKA is also overexpressed in diverse solid tumors,[4] the potential clinical applications of this approach are widespread. Further studies are therefore warranted to investigate the safety and utility of this novel therapy in the clinic.

Acknowledgments

The authors are grateful for the skilled technical assistance of Dr Kenji Kameda, Ehime University, Japan. They also thank Dr Midori Okumura and Dr Tomihiro Katayama, Department of Obstetrics and Gynecology, Ehime University Graduate School of Medicine, Japan, for supplying cord blood samples; Dr Hiroo Saji, HLA Laboratory, Japan, for HLA typing, Dr Erik Hooijberg; Vrije Universiteit Medisch Centrum, The Netherlands, for supplying the Jurkat/MA cell line; and Dr A. John Barrett, National Heart, Lung, and Blood Institute, National Institutes of Health, for supplying the C1R-A2 cell line.

This work was supported in part by grants from the Ministry of Education, Culture, Sports, Science and Technology of Japan to T.O., H.F., and M.Y., a Grant-in-Aid for Cancer Research from the Ministry of Health, Labor and Welfare to M.Y., and a grant from the Third Term Comprehensive Control Research for Cancer to K.K. D.A.P. is a Medical Research Council (United Kingdom) Senior Clinical Fellow.

Authorship

Contribution: K.N. and T.O. performed the research and wrote the paper; H.F. designed and performed the research, wrote and edited the paper, and provided financial support; J.A., T.S., J.M., H.S., J.J.M., and E.I. discussed and interpreted the experimental results and provided materials; K.K., E.G., and D.A.P. made and supplied the tetramers and edited the paper; and M.Y. discussed and interpreted the experimental results, edited the paper, and provided financial support.

Conflict-of-interest disclosure: The authors declare no competing financial interests.

Correspondence: Hiroshi Fujiwara, Department of Bioregulatory Medicine, Ehime University Graduate School of Medicine, Toon, Ehime 791-0295, Japan; e-mail: yunarief@m.ehime-u.ac.jp; or Masaki Yasukawa, Department of Bioregulatory Medicine, Ehime University Graduate School of Medicine, Toon, Ehime 791-0295, Japan; e-mail: yasukawa@m.ehime-u.ac.jp.

References

1. Marumoto T, Zhang D, Saya H. Aurora-A-a guardian of poles. *Nat Rev Cancer.* 2005;5(1):42-50.
2. Carmena M, Earnshaw WC. The cellular geography of aurora kinases. *Nat Rev Mol Cell Biol.* 2003;4(11):842-845.
3. Bischoff JR, Anderson L, Zhu Y, et al. A homologue of Drosophila aurora kinase is oncogenic and amplified in human colorectal cancers. *EMBO J.* 1998;17(11):3052-3065.
4. Gautschi O, Heighway J, Mack PC, Pumell PR, Lara PN Jr, Gandara DR. Aurora kinases as an anticancer targets. *Clin Cancer Res.* 2008;14(6):1639-1648.
5. Ikezoe T, Yang J, Nishioka C, et al. A novel treatment strategy targeting Aurora kinases in acute myelogenous leukemia. *Mol Cancer Ther.* 2007;6(6):1851-1857.
6. Ochi T, Fujiwara H, Suemori K, et al. Aurora-A kinase: a novel target of cellular immunotherapy for leukemia. *Blood.* 2009;113(1):66-74.
7. Ewart-Toland A, Briassouli P, de Koning JP, et al. Identification of Stk6/STK15 as a candidate low-penetrance tumor-susceptibility gene in mouse and human. *Nat Genet.* 2003;34(4):403-412.
8. Xu HT, Ma L, Qi FJ, et al. Expression of serine threonine kinase 15 is associated with poor differentiation in lung squamous cell carcinoma and adenocarcinoma. *Pathol Int.* 2006;56(7):375-380.
9. Boss DS, Beijnen JH, Schellens JH. Clinical experience with aurora kinase inhibitors: a review. *Oncologist.* 2009;14(8):780-793.
10. Dees EC, Infante JR, Cohen RB, et al. Phase 1 study of MLN8054, a selective inhibitor of Aurora A kinase in patients with advanced solid tumors. *Cancer Chemother Pharmacol.* 2011;67(4):945-954.
11. Steeghs N, Eskens FA, Gelderblom H, et al. Phase I pharmacokinetic and pharmacodynamic study of the aurora kinase inhibitor danusertib in patients with advanced or metastatic solid tumors. *J Clin Oncol.* 2009;27(30):5094-5101.
12. Traynor AM, Hewitt M, Liu G, et al. Phase I dose escalation study of MK-0457, a novel Aurora kinase inhibitor, in adult patients with advanced solid tumors. *Cancer Chemother Pharmacol.* 2011;67(2):305-314.
13. Hamada M, Yakushijin Y, Ohtsuka M, Kakimoto M, Yasukawa M, Fujita S. Aurora2/BTAK/STK15 is involved in cell cycle checkpoint and cell survival of aggressive non-Hodgkin's lymphoma. *Br J Haematol.* 2003;121(3):439-447.
14. Kobayashi H, Azumi M, Hayashi S, et al. Characterization of human CD4 helper T cell responses against Aurora kinase A. *Cancer Immunol Immunother.* 2010;59(7):1029-1039.
15. Morgan RA, Dudley ME, Wunderlich JR, et al. Cancer regression in patients after transfer of genetically engineered lymphocytes. *Science.* 2006;314(5796):126-129.
16. Johnson LA, Morgan RA, Dudley ME, et al. Gene therapy with human and mouse T-cell receptors mediates cancer regression and targets normal tissues expressing cognate antigen. *Blood.* 2009;114(3):535-546.
17. Bendle GM, Linnemann C, Hooijkaas AI, et al. Lethal graft-versus-host disease in mouse models of T cell receptor gene therapy. *Nat Med.* 2010;16(5):565-570.
18. Okamoto S, Mineno J, Ikeda H, et al. Improved expression and reactivity of transduced tumor-specific TCRs in human lymphocytes by specific silencing of endogenous TCR. *Cancer Res.* 2009;69(23):9003-9011.
19. Robbins PF, Morgan RA, Feldman SA, et al. Tumor regression in patients with metastatic synovial cell sarcoma and melanoma using genetically engineered lymphocytes reactive with NY-ESO-1. *J Clin Oncol.* 2011;29(7):917-924.
20. Calogero A, Hospers GA, Krüse KM, et al. Retargeting of a T cell line by anti MAGE-3/HLA-A2 alpha beta TCR gene transfer. *Anticancer Res.* 2000;20(3A):1793-1799.
21. Price DA, Brenchly JM, Ruff LE, et al. Avidity for antigen shapes clonal dominance in CD8+ T cell populations specific for persistent DNA viruses. *J Exp Med.* 2005;202(10):1349-1361.
22. Kuzushima K, Hayashi N, Kimura H, Tsurumi T. Efficient identification of HLA-A*2402-restricted cytomegalovirus-specific $CD8^+$ T-cell epitopes by a computer algorithm and an enzyme-linked immunospot assay. *Blood.* 2001;98(6):1872-1881.
23. Ohminami H, Yasukawa M, Fujita S. HLA class I-restricted lysis of leukemia cells by a $CD8^+$ cytotoxic T-lymphocyte clone specific for WT1 peptide. *Blood.* 2000;95(1):286-293.
24. Tsuji T, Yasukawa M, Matsuzaki J, et al. Generation of tumor-specific, HLA class I-restricted human Th1 and Tc1 cells by cell engineering with tumor peptide-specific T-cell receptor genes. *Blood.* 2005;106(2):470-476.
25. Folch G, Scaviner D, Contet V, Lefranc MP. Protein displays of the human T cell receptor alpha, beta, gamma and delta variable and joining regions. *Exp Clin Immunogenet.* 2000;17(4):205-215.
26. Arden B, Clark SP, Kabelitz D, Mak TW. Human T-cell receptor variable gene segment families. *Immunogenetics.* 1995;42(6):455-500.
27. Jedema I, van der Werff NM, Barge RM, Willemze R, Falkenburg JH. New CFSE-based assay to determine susceptibility to lysis by cytotoxic T cells of leukemic precursor cells within a heterogeneous target cell population. *Blood.* 2004;103(7):2677-2682.
28. Yasukawa M, Ohminami H, Arai J, Kasahara Y, Ishida Y, Fujita S. Granule exocytosis, and not the fas/fas ligand system, is the main pathway of cytotoxicity mediated by alloantigen-specific $CD4^+$ as well as $CD8^+$ cytotoxic T lymphocytes in humans. *Blood.* 2000;95(7):2352-2355.
29. Ito M, Hiramatsu H, Kobayashi K, et al. NOD/SCID/gamma(c) (null) mouse: an excellent recipient mouse model for engraftment of human cells. *Blood.* 2002;100(9):3175-3182.
30. Xue SA, Gao L, Hart D, at al. Elimination of human leukemia cells in NOD/SCID mice by WT1-TCR gene-transduced human T cells. *Blood.* 2005;106(9):3062-3067.
31. Finney HM, Akbar AN, Lawson AD. Activation of

resting human primary T cells with chimeric receptors: costimulation from CD28, inducible costimulator, CD134, and CD137 in series with signals from the TCR zeta chain. *J Immunol.* 2004; 172(1):104-113.

32. Brentjens RJ, Santos E, Nikhamin Y, et al. Genetically targeted T cells eradicate systemic acute lymphoblastic leukemia xenografts. *Clin Cancer Res.* 2007;13(18 Pt 1):5426-5435.
33. Hollyman D, Stefanski J, Przybylowski M, et al. Manufacturing validation of biologically functional T cells targeted to CD19 antigen for autologous adoptive cell therapy. *J Immunother.* 2009;32(2): 169-180.
34. Wang J, Press OW, Lindgren CG, et al. Cellular immunotherapy for follicular lymphoma using genetically modified CD20-specific $CD8^+$ cytotoxic T lymphocytes. *Mol Ther.* 2004;9(4):577-586.
35. James SE, Greenberg PD, Jensen MC, et al. Antigen sensitivity of CD22-specific chimeric TCR is modulated by target epitope distance from the cell membrane. *J Immunol.* 2008;180(10):7028-7038.
36. Hombach A, Muche JM, Gerken M, et al. T cells engrafted with a recombinant anti-CD30 receptor target autologous $CD30^+$ cutaneous lymphoma cells. *Gene Ther.* 2001;8(11):891-895.
37. Hudecek M, Schmitt TM, Baskar S, et al. The B-cell tumor-associated antigen ROR1 can be targeted with T cells modified to express a ROR1-specific chimeric antigen receptor. *Blood.* 2010; 116(22):4532-4541.
38. Till BG, Jensen MC, Wang J, et al. Adoptive immunotherapy for indolent non-Hodgkin lymphoma and mantle cell lymphoma using genetically modified autologous CD20-specific T cells. *Blood.* 2008;112(6):2261-2271.
39. Offringa R. Antigen choice in adoptive T-cell therapy of cancer. *Curr Opin Immunol.* 2009; 21(2):190-199.
40. Moore AS, Blagg J, Linardopoulos S, Pearson ADJ. Aurora kinase inhibitors: novel small molecules with promising activity in acute and Philadelphia-positive leukemias. *Leukemia.* 2010;24: 671-678.
41. Ye D, Garcia-Manero G, Kantarjian HM, et al. Analysis of Aurora kinase A expression in $CD34^+$ blast cells isolated from patients with myelodysplastic syndromes and acute myeloid leukemia. *J Hematop.* 2009;2(1):2-8.
42. Misaghian N, Ligresti G, Steelman LS, et al. Targeting the leukemic stem cell: the Holy Grail of leukemia therapy. *Leukemia.* 2009;23(1):25-42.
43. Jin L, Lee EM, Ramshaw HS, et al. Monoclonal antibody-mediated targeting of CD123, IL-3 receptor alpha chain, eliminates human acute myeloid leukemic stem cells. *Cell Stem Cell.* 2009; 5(1):31-42.
44. Kikushige Y, Shima T, Takayanagi S, et al. TIM-3 is a promising target to selectively kill acute myeloid leukemia stem cells. *Cell Stem Cell.* 2010; 7(6):708-717.
45. Saito Y, Kitamura H, Hijikata A, et al. Identification of therapeutic targets for quiescent, chemotherapy-resistant human leukemia stem cells. *Sci Transl Med.* 2010;2(17):17ra9.
46. Ochi T, Fujiwara H, Okamoto S, et al. Novel adoptive T-cell immunotherapy using a WT1-specific TCR vector encoding silencers for endogenous TCRs show marked antileukemia reactivity and safety. *Blood.* 2011;118(6):1495-1503.
47. Morris EC, Tsallios A, Bendle GM, Xue SA, Stauss HJ. A critical role of T cell antigen receptor-transduced MHC class I-restricted helper T cells in tumor protection. *Proc Natl Acad Sci U S A.* 2005;102(22):7934-7939.
48. Ray S, Chhabra A, Chakraborty NG, et al. MHC-I-restricted melanoma antigen specific TCR-engineered human $CD4^+$ T cells exhibit multifunctional effector and helper responses, in vitro. *Clin Immunol.* 2010;136(3):338-347.
49. Ly LV, Sluijter M, Versluis M, et al. Peptide vaccination after T-cell transfer causes massive clonal expansion, tumor eradication, and manageable cytokine storm. *Cancer Res.* 2010;70(21):8339-8346.

Cancer Research

Intracellular Tumor-Associated Antigens Represent Effective Targets for Passive Immunotherapy

Takuro Noguchi[1,4,8], Takuma Kato[2], Linan Wang[1,3], Yuka Maeda[1,5], Hiroaki Ikeda[3], Eiichi Sato[6], Alexander Knuth[7], Sacha Gnjatic[5,8], Gerd Ritter[8], Shimon Sakaguchi[5], Lloyd J. Old[†], Hiroshi Shiku[1,3], and Hiroyoshi Nishikawa[1,5]

Abstract

Monoclonal antibody (mAb) therapy against tumor antigens expressed on the tumor surface is associated with clinical benefit. However, many tumor antigens are intracellular molecules that generally would not be considered suitable targets for mAb therapy. In this study, we provide evidence challenging this view through an investigation of the efficacy of mAb directed against NY-ESO-1, a widely expressed immunogen in human tumors that is expressed intracellularly rather than on the surface of cells. On their own, NY-ESO-1 mAb could neither augment antigen-specific $CD8^+$ T-cell induction nor cause tumor eradication. To facilitate mAb access to intracellular target molecules, we combined anti-NY-ESO-1 mAb with anticancer drugs to accentuate the release of intracellular NY-ESO-1 from dying tumor cells. Strikingly, combination therapy induced a strong antitumor effect that was accompanied by the development of NY-ESO-1–specific effector/memory $CD8^+$ T cells that were not elicited by single treatments alone. The combinatorial effect was also associated with upregulation of maturation markers on dendritic cells, consistent with the organization of an effective antitumor T-cell response. Administration of Fc-depleted F(ab) mAb or combination treatment in Fcγ receptor–deficient host mice abolished the therapeutic effect. Together, our findings show that intracellular tumor antigens can be captured by mAbs and engaged in an efficient induction of $CD8^+$ T-cell responses, greatly expanding the possible use of mAb for passive cancer immunotherapy. *Cancer Res; 72(7); 1672–82. ©2012 AACR.*

Introduction

With the molecular identification of tumor antigens recognized by the human immune system, antigen-specific immunotherapy for cancers has been developed and is explored in the clinic (1–3). Particularly, monoclonal antibodies (mAb) that recognize surface antigens, such as trastuzumab (anti-Her2/neu) and rituximab (anti-CD20), as a single agent or in combination with chemotherapy, are used in the clinic for frontline or salvage therapy and have resulted in objective and durable clinical responses (3–5). One of the major therapeutic mechanisms of mAb is considered to be the selective interruption of vital signaling pathways in which the targeted antigens are critically involved (3, 5). In addition, there is accumulating evidence that mAb therapy also works through antibody-dependent cellular cytotoxicity (ADCC) by natural killer (NK) cells or through the activation of complement, both of which depend on the Fc portion of the mAbs (6–9). Furthermore, Fc receptor–mediated uptake of immune complexes results in activation of antigen-presenting cells (APC) and facilitates cross-presentation of those antigens to tumor-specific $CD8^+$ T cells and inhibition of tumor growth, as was shown recently in HER2/*neu* and melanoma differentiation antigen tyrosinase–related protein-1 (Trp1; gp75) models (10–13).

However, many well-characterized tumor-associated antigens, including cancer/testis (CT) antigens, are intracellular antigens and thus not accessible for antibodies (14–16). An exception is mAb TA99, which targets gp75 and was shown to induce NK and $CD4^+$ T-cell–dependent antitumor responses *in vivo* (17). However, the fact that gp75 is expressed both on the cell surface and intracellularly makes it difficult to define the precise targets for the antitumor responses induced by mAb TA99 (12, 17).

NY-ESO-1, a CT antigen discovered by SEREX (serologic identification of antigens by recombinant expression cloning) using the serum of a patient with esophageal cancer, is frequently expressed in cancer cells of various tissue origins

Authors' Affiliations: Departments of [1]Cancer Vaccine, [2]Cellular and Molecular Immunology, and [3]Immuno-Gene Therapy, Mie University Graduate School of Medicine, Mie; [4]Department of Surgical Oncology, Hokkaido University Graduate School of Medicine, Hokkaido; [5]Experimental Immunology, Immunology Frontier Research Center, Osaka University, Osaka; [6]Department of Anatomic Pathology, Tokyo Medical University, Tokyo, Japan; [7]Department of Oncology, University Hospital Zurich, Zurich, Switzerland; and [8]Ludwig Institute for Cancer Research, New York Branch, Memorial Sloan-Kettering Cancer Center, New York

Note: Supplementary data for this article are available at Cancer Research Online (http://cancerres.aacrjournals.org/).

† Deceased.

Corresponding Authors: Hiroyoshi Nishikawa, Experimental Immunology, Immunology Frontier Research Center, Osaka University, 3-1 Yamadaoka, Suita, Osaka 565-0871, Japan. Phone: 81-6-6879-4963; Fax: 81-6-6879-4464; E-mail: nisihiro@ifrec.osaka-u.ac.jp; and Hiroshi Shiku, Departments of Cancer Vaccine and Immuno-Gene Therapy, Mie University Graduate School of Medicine, 2-174 Edobashi, Tsu, Mie 514-8507, Japan. Phone: 81-59-231-5062; Fax: 81-59-231-5276; E-mail: shiku@clin.medic.mie-u.ac.jp

doi: 10.1158/0008-5472.CAN-11-3072

but not in normal somatic cells except for germ cells in the testis (2, 18). Spontaneous cellular and humoral immune responses against NY-ESO-1 are found in patients with cancer, which underscores its immunogenicity (2, 18). It has an intracellular location and lacks cell surface expression (2, 18), thus curtails it from being a candidate of mAb therapy. Interestingly, NY-ESO-1 protein/IgG antibody complexes (immune complexes, IC) are efficiently cross-presented to the MHC class I pathway (19, 20) and there is a close correlation between antibody and $CD8^+$ T-cell responses (2, 21), suggesting that NY-ESO-1–specific $CD8^+$ T-cell induction by cross-priming *in vivo* is associated with the induction of specific antibodies. These data prompted us to analyze the possibility whether mAb therapy could be applied to an intracellular molecule NY-ESO-1 and inhibit tumor growth by enhancing $CD8^+$ T-cell induction.

We have established syngeneic tumor models in BALB/c mice using CT26 colon carcinoma cells and CMS5a sarcoma cells that are stably transfected with NY-ESO-1 (22, 23). Using these models, we addressed whether NY-ESO-1 mAb combined with chemotherapy augmented NY-ESO-1–specific $CD8^+$ T-cell induction and inhibited tumor growth.

Materials and Methods

Mice

Female BALB/c mice and BALB/$c^{nu/nu}$ mice were obtained from SLC Japan or Jackson laboratory and used at 7 to 10 weeks of age. BALB/c mice deficient in the γ-chain subunit of Fc receptors were obtained from Taconic and used at 7 to 10 weeks of age. Mice were maintained in accordance with the NIH and American Association of Laboratory Animal Care Regulations. The experimental protocol was approved by the Ethics Review Committee for Animal Experimentation of Mie University Graduate School of Medicine (Mie, Japan) and by the Memorial Sloan-Kettering Cancer Center Institutional Animal Care and Use Committee (New York, NY).

Tumors

CT26 is a colon epithelial tumor derived by intrarectal injections of *N*-nitroso-*N*-methylurethane in BALB/c mice (24). CT26 expressing NY-ESO-1 (CT26-NY-ESO-1) was established as described previously (23). CMS5a is a subcloned cell line obtained from CMS5 (25). CMS5a-NY-ESO-1 was established as described previously (22).

Antibodies and reagents

Anti-NY-ESO-1 mAbs [E978 (mouse IgG1) recognizing NY-ESO-1_{71-90}, ES121 (mouse IgG1) recognizing NY-ESO-1_{91-110}, 219–510 (mouse IgG1) recognizing NY-ESO-1_{21-40} (Supplementary Fig. S3; ref. 26)]; anti-CD4 (GK1.5, rat IgG2b), anti-CD8 (19/178, mouse IgG2a), and anti-MAGE-A4 (MCV1, mouse IgG1) were purified from hybridoma supernatant by protein G affinity chromatography. The F(ab) fragment of E978 was generated using the ImmunoPure Fab Preparation Kit (Thermo Fisher Scientific). Anti-CD8 (53–6.7), anti-CD45RB (16A), anti-CD80 (16-10A1), anti-CD86 (GL-1), anti-CD40 (3/23), anti-IFN-γ (XMG1.2), anti-CD62L (MEL-14), anti-CD11c (HL3), anti-TNF-α (MP6-XT22), and antimouse IgG1 (A85-1) mAbs were purchased from BD Biosciences, Biolegend, or eBioscience. Phycoerythrin (PE)-labeled NY-ESO-1_{81-88}-D^d tetramers were provided by Drs. P. Guillaume and I. Luescher (Ludwig Institute Core Facility, Lausanne, Switzerland). An anti-NY-ESO-1 human IgG1 mAb (12D7) was obtained from CT Atlantic. p63 (T) peptide TYLPTNASL (27), AH-$1_{138-147}$ peptide SPSYVHQF (28), and NY-ESO-1_{81-88} peptide RGPESRLL (23) were purchased from Operon Biotechnologies and BioSynthesis and Sigma.

Chemotherapeutic agents

5-Fluorouracil (5-FU; Kyowa Hakko Kirin,), doxorubicin (Kyowa Hakko Kirin), CPT-11 (Yakult), and paclitaxel (Bristol-Myers Squibb) were injected intraperitoneally as indicated.

Tumor challenge

Mice were inoculated with 0.5×10^6 to 1×10^6 CT26-NY-ESO-1 cells, 1×10^6 CMS5a-NY-ESO-1, or 1×10^6 CT26-MAGE-A4 cells in the right hind flank subcutaneously. Mice were monitored 3 times a week and were sacrificed when tumors reached greater than 20 mm.

Staining and flow cytometry

To collect tumor-infiltrating T cells, tumors were minced and treated with 1 mg/mL of collagenase IA (Sigma) in Hanks' balanced salt solution (HBSS) for 90 minutes at room temperature.

Cells harvested from draining lymph node (dLN) and tumors were stained for surface markers in PBS with 0.5% FBS for 15 minutes at 4°C. For intracellular cytokine staining, 1×10^6 to 3×10^6 cells from tumors or dLNs were cultured with peptide for 5 hours at 37°C, and GolgiPlug was added for the last 4 hours of culture. These cells were stained for surface markers and intracellularly with allophycocyanin-conjugated anti-IFN-γ and PE-conjugated anti-TNF-α mAbs after permeabilization and fixation using Cytofix/Cytoperm Kit (BD Bioscience). Dead cells were excluded by LIVE/DEAD Fixable Dead Cell Stain Kits (Invitrogen). Cells were analyzed on FACSCanto or FACSCalibur (BD Bioscience) and FlowJo software (Tree Star).

Fluorescent immunohistochemistry

Three micrometers of tissue sections prepared from fresh-frozen tumor specimens were fixed with ice-chilled acetone for 15 minutes. Alexa 488–labeled antihuman IgG antibody (Invitrogen) was applied and incubated at room temperature for 2 hours. For double immunolabeling, sections were fixed with 3% paraformaldehyde for 15 minutes, incubated with anti-cleaved caspase-3 (Cell Signaling Technology) at room temperature for 2 hours and then incubated with Alexa 488–labeled anti-human IgG antibody and Alexa 568–labeled antirabbit IgG Ab (Invitrogen) at room temperature for 2 hours. Sections were rinsed with PBS, counterstained with 4′,6-diamidino-2-phenylindole (DAPI), and mounted. Images were captured using ×40 magnification objective by Zeiss Axiocam system (Carl Zeiss).

Statistical analysis

Tumor curves were assessed by one-way ANOVA with a Bonferroni multiple comparisons posttest. Single measurement

comparison between 2 groups was evaluated by 2-sided Student *t* test. *P* values <0.05 were considered statistically significant.

Results

Establishment of CT26-NY-ESO-1

We established a syngeneic colon carcinoma model (CT26-NY-ESO-1) with stable NY-ESO-1 expression (2, 22, 23). NY-ESO-1 expression in CT26-NY-ESO-1 cells was exclusively intracellular, and no NY-ESO-1 protein was detected on the cell surface (Supplementary Fig. S1A), consistent with the expression of NY-ESO-1 protein in human cancer cells (2). These CT26-NY-ESO-1 cells maintained the same tumor growth capacity as their parental CT26 cells in both wild-type Balb/c and C.B-17 SCID (severe combined immunodeficient) mice, indicating that there was no alteration of tumorigenicity caused by the NY-ESO-1 transfection (Supplementary Fig. S1B). When BALB/c mice were inoculated with CT26-NY-ESO-1 cells, spontaneous antibody and $CD8^+$ T-cell responses were detected after 7 days and increased thereafter (Supplementary Fig. S1C and S1D). These spontaneous immune responses closely paralleled spontaneous NY-ESO-1–specific immune responses found in humans (2).

We used this tumor model to explore the antitumor effects of mAbs against NY-ESO-1 alone and in combination with an anticancer drug. To select anticancer drugs suitable for this model, we examined the antitumor capacity of several anticancer drugs (5-FU, CPT-11, paclitaxel, and doxorubicin) against CT26-NY-ESO-1. Of the 4 drugs, 5-FU exhibited a significant antitumor effect (Supplementary Fig. S2A). When CT26-NY-ESO-1 cells were cultured with 5-FU, NY-ESO-1 protein was released from CT26-NY-ESO-1 cells into the culture supernatant but not from parental CT26 cells (Supplementary Fig. S2B). On the basis of these data, we chose 5-FU for our further experiments.

Combination treatment with anti-NY-ESO-1 mAb and 5-FU results in augmented tumor growth inhibition

BALB/c mice were inoculated with CT26-NY-ESO-1 and were injected with 5-FU (75 mg/kg) and anti-NY-ESO-1 mAb (clone; E978, 100 μg, 2 days after 5-FU injection) when the tumor was palpable (around 25 mm^2). Treatment was repeated after 1 week. The combination treatment with anti-NY-ESO-1 mAb and 5-FU exhibited a significantly augmented antitumor effect and longer survival compared with control mice or mice that had received either 5-FU or anti-NY-ESO-1 mAb alone (Fig. 1A and B). This augmented antitumor effect was also observed when another anti-NY-ESO-1 mAb (clone; ES121, 100 μg) was used, but not with a control mAb, against another immunogenic CT antigen MAGE-A4, which is not expressed in the CT26-NY-ESO-1 cells (Fig. 1C and D). In contrast, combination treatment with anti-MAGE-A4 mAb (clone; MCV1, 100 μg), but not control antibody and 5-FU, exhibited an augmented antitumor effect against CT26-MAGE-A4 (Fig. 1E). To show that the effect of this combination treatment is not limited to the CT26, we examined the antitumor effect using CMS5a fibrosarcoma cells. BALB/c mice were inoculated with CMS5a-NY-ESO-1 and were injected with doxorubicin (50 μL intratumoral injection, 0.25 mmol/L) and anti-NY-ESO-1 mAb. As systemic administration of doxorubicin did not induce effective killing of CMS5a-NY-ESO-1, we used an intratumoral injection method. This combination treatment with anti-NY-ESO-1 mAb (but not an isotype control antibody) and doxorubicin exhibited a significantly augmented antitumor effect as well (Fig. 1F). These data suggest that the augmented antitumor effect is an antigen-specific phenomenon and that this combination treatment could be applicable to a broader range of intracellular antigens and tumors.

We next investigated whether a cocktail of 2 different anti-NY-ESO-1 mAbs (E978 50 μg and ES121 50 μg) that recognize 2 different nonoverlapping epitopes on the NY-ESO-1 protein (Supplementary Fig. S3) further augmented antitumor effects. We observed no additive antitumor effects when mice were treated with the combination of 2 different anti-NY-ESO-1 mAbs and 5-FU compared with mice treated with a single anti-NY-ESO-1 mAb and 5-FU (Fig. 1G).

Augmented tumor growth inhibition by combination treatment with anti-NY-ESO-1 mAb and 5-FU is dependent on $CD8^+$ T cells

To gain insight into the cellular components involved in the augmented antitumor effects by the combination treatment, we initially examined the role of T cells using BALB/$c^{nu/nu}$ mice. BALB/$c^{nu/nu}$ mice were inoculated with CT26-NY-ESO-1 and combination treatment with 5-FU and anti-NY-ESO-1 mAb was initiated when the tumor was palpable. The augmented antitumor effect by the combination treatment in wild-type BALB/c mice was abrogated in BALB/$c^{nu/nu}$ mice (Fig. 2A).

Given the critical role of T cells in this augmentation of antitumor effects, we next explored the outcome of $CD4^+$/$CD8^+$ T-cell depletion on the augmented antitumor effect. BALB/c mice bearing CT26-NY-ESO-1 tumors were injected with 5-FU and anti-NY-ESO-1 mAb and received anti-CD4 (days 7, 14, and 21) or anti-CD8 mAb (days 7 and 21). The depletion of $CD8^+$ T cells totally abolished the augmented antitumor effects (Fig. 2B). In contrast, $CD4^+$ T-cell depletion did not affect the augmented antitumor effects (Fig. 2B).

Combination treatment with anti-NY-ESO-1 mAb and 5-FU enhances NY-ESO-1–specific $CD8^+$ T-cell induction

Considering a critical role of $CD8^+$ T cells, we examined NY-ESO-1–specific T cells in dLNs. BALB/c mice were inoculated with CT26-NY-ESO-1 and received the combination treatment. dLNs and tumors were harvested on days 14 to 16, and cells were incubated with NY-ESO-1_{81-88} (23) or control peptide, and cytokine secretion was analyzed. Combination treatment with anti-NY-ESO-1 mAb and 5-FU elicited significantly higher numbers of NY-ESO-1–specific $CD8^+$ T cells producing IFN-γ and/or TNF-α than 5-FU alone (Fig. 3A). Furthermore, there was a trend of higher numbers of NY-ESO-1–specific $CD8^+$ T cells in tumors treated with the combination treatment than those treated with 5-FU alone (Fig. 3C).

To explore further differences in NY-ESO-1_{81-88}–specific $CD8^+$ T cells, the effector/memory status was analyzed. The

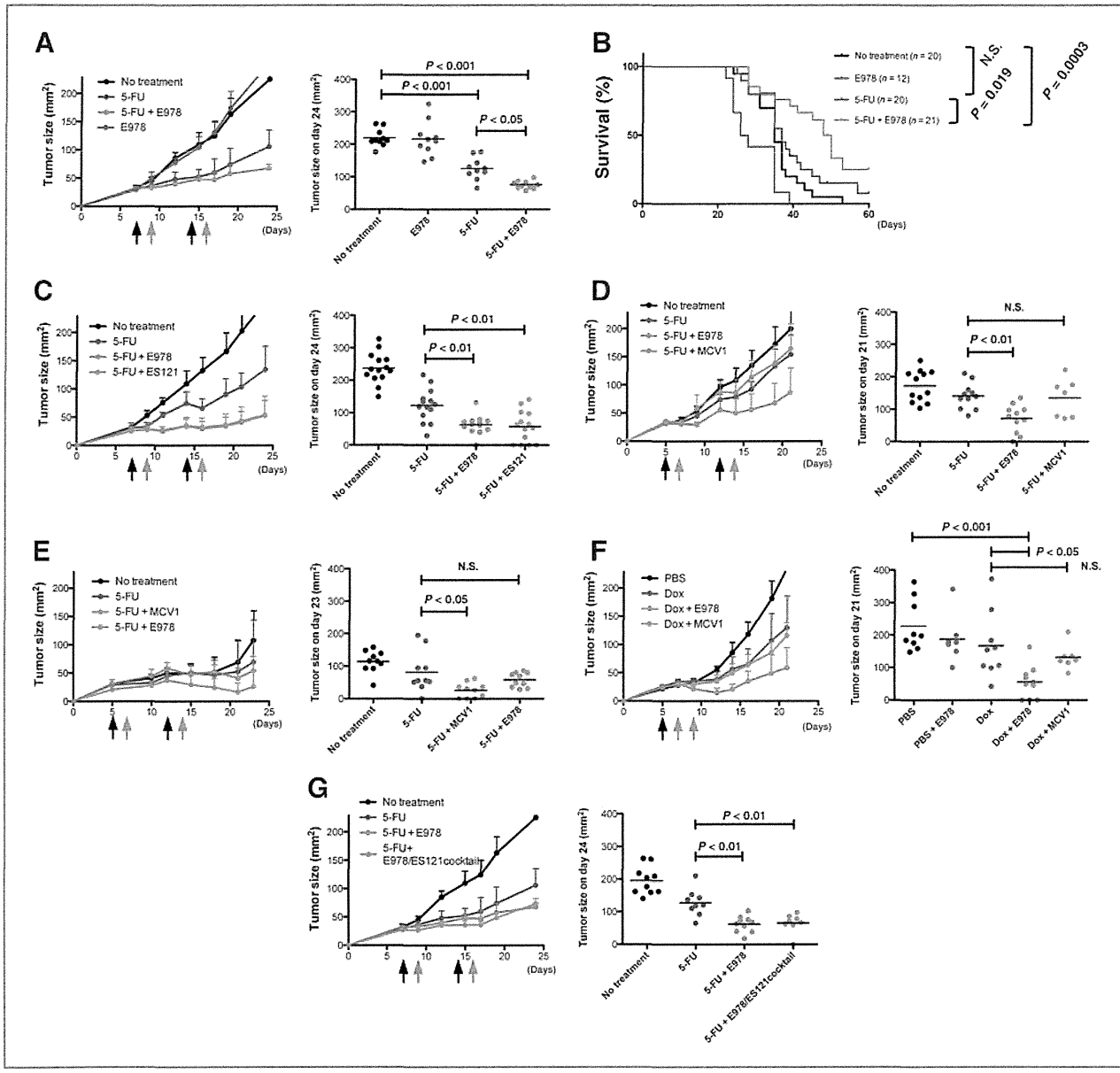

Figure 1. Combination of mAb and an anticancer drug exhibits augmented tumor growth inhibition. A–D and G, BALB/c mice were inoculated with CT26-NY-ESO-1 and treatment was started when tumors were palpable (around 25 mm^2, days 5–7). Mice received 5-FU intraperitoneally (black arrow) and/or anti-NY-ESO-1 mAb (clone; E978 or ES121) or anti-MAGE-A4 mAb (clone; MCV1) 2 days after 5-FU injection (red arrow). Treatment was repeated twice at 1-week intervals. A, left, tumor growth curves representative of 2 independent experiments; right, summary of tumor size on day 24 of 2 independent experiments. B, survival rate curves summarized from another 3 independent experiments (separate from tumor growth data) are shown. C and D, left, tumor growth curves representative of 2 independent experiments. Right, summary of tumor size of 2 independent experiments on days 24 and 21, respectively. E, BALB/c mice were inoculated with CT26-MAGE-A4 and treatment was started as in A. Mice received 5-FU (black arrow) and anti-MAGE-A4 mAb (clone; MCV1) or anti-NY-ESO-1 mAb (clone; E978) 2 days after 5-FU injection (red arrow). Left, tumor growth curves representative of 2 independent experiments; right, summary of tumor size on day 23 of 2 independent experiments. F, BALB/c mice were inoculated with CMS5a-NY-ESO-1 and treatment was started as in A. Mice received doxorubicin (Dox; 50 μL, 0.25 mmol/L) intratumorally (black arrow) and/or anti-NY-ESO-1 mAb (clone; E978) 2 and 4 days after doxorubicin administration (red arrow). Left, tumor growth curves representative of 2 independent experiments; right, summary of tumor size on day 21 of 2 independent experiments. G, mice were injected with 5-FU (black arrow) and anti-NY-ESO-1 mAb (E978, 100 μg) or cocktail of 2 anti-NY-ESO-1 mAbs (E978 50 μg and ES121 50 μg) 2 days after 5-FU injection (red arrow). Left, tumor growth curves representative of 2 independent experiments; right, summary of tumor size on day 24 of 2 independent experiments. Tumor size was monitored 3 times a week. Each group consisted of 3 to 8 mice. Data are presented as mean ± SD. N.S., not significant.

frequency of NY-ESO-1–specific $CD8^+$ T cells as measured by $CD8^+$NY-ESO-1/D^d $tetramer^+$ T cells was higher in mice treated with the combination therapy than in mice treated with 5-FU alone, confirming the data from the intracellular cytokine assays. The frequency of effector/memory ($CD62L^{low}CD45RB^{low}$) T cells was higher in mice treated with

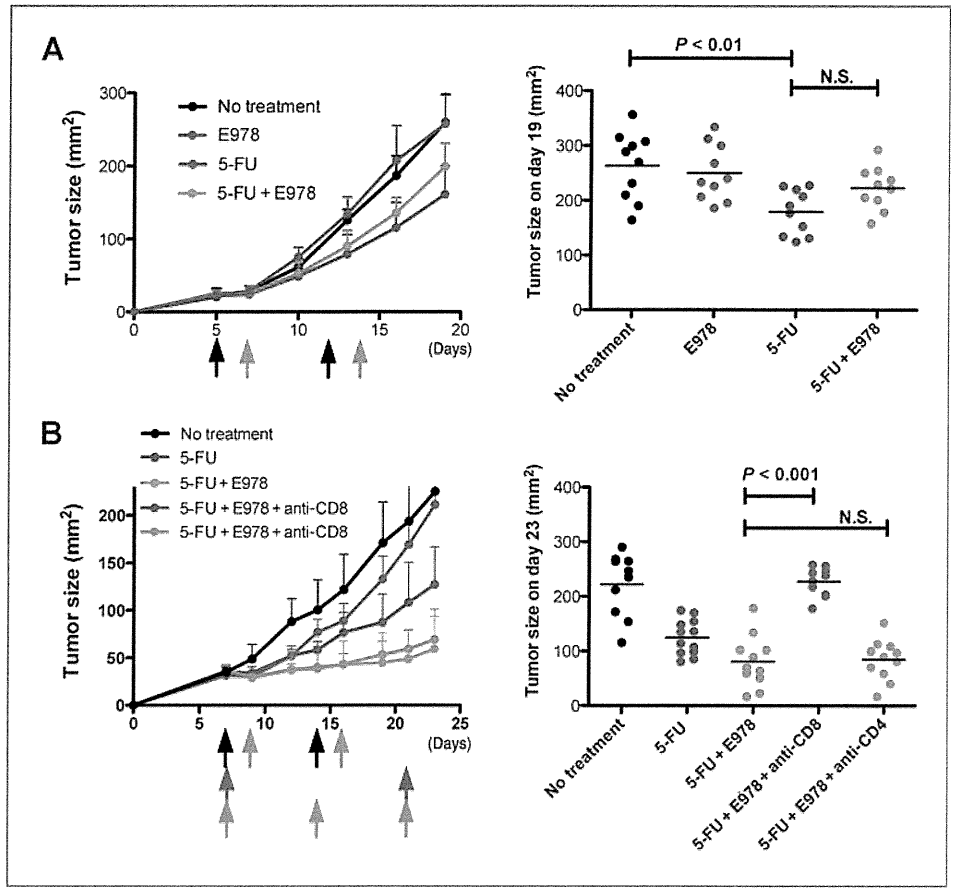

Figure 2. Augmented tumor growth inhibition by the combination treatment depends on CD8$^+$ T cells. A, BALB/c$^{nu/nu}$ mice were inoculated with CT26-NY-ESO-1 and treatment with 5-FU (days 5 and 12; black arrow) and anti-NY-ESO-1 mAb (E978, days 7 and 14; red arrow) was started as in Fig. 1A. Left, tumor growth curves representative of 2 independent experiments; right, summary of tumor size on day 19 of 2 independent experiments. B, BALB/c mice bearing CT26-NY-ESO-1 were injected with 5-FU (days 7 and 14; black arrow) and anti-NY-ESO-1 mAb (E978, days 9 and 16; red arrow) and received anti-CD4 (days 7, 14, and 21; brown arrow) or anti-CD8 mAb (days 7 and 21; purple arrow), resulting in more than 95% depletion of CD4/CD8 cell depletion. Left, tumor growth curves representative of 2 independent experiments; right, summary of tumor size on day 23 of 2 independent experiments. Tumor size was monitored 3 times a week. Each group consisted of 5 to 7 mice. Data are presented as mean ± SD. N.S., not significant.

the combination treatment (Fig. 3B). In contrast, frequency of naive (CD62L^{high}CD45RB^{high}) T cells was higher in mice treated with 5-FU alone, indicating that the combination treatment efficiently activated antigen-specific CD8$^+$ T cells.

Therapeutically effective antigen spreading is observed in mice treated with the combination treatment

Certain immunization strategies result in the development of an immune response against tumor antigens that are not contained in the vaccine but are found in tumor cells, a phenomenon known as antigen spreading (22, 29, 30). Therefore, we explored whether the combination treatment resulted in the development of an immune response against other antigens expressed in tumor cells. As we used CT26 tumors, we examined CD8$^+$ T cells recognizing AH-1 peptide, which is derived from the envelope protein (gp70) of an endogenous ecotropic murine leukemia provirus expressed by CT26 and previously shown to be a target of CD8$^+$ T cells (28). Mice bearing CT26-NY-ESO-1 received treatment with anti-NY-ESO-1 mAb and 5-FU. Given that antigen spreading is observed after the antigen release from killed tumor cells, AH-1–specific CD8$^+$ T-cell induction was analyzed at later time point (day 24). Significantly higher numbers of AH-1–specific CD8$^+$ T cells was detected in mice treated with anti-NY-ESO-1 mAb and 5-FU than in mice treated with 5-FU alone (Fig. 4).

The antibody–Fc portion is required for the augmented antitumor effect by the combination treatment

We next explored the mechanism(s) of the augmented antitumor effect and the differences of NY-ESO-1_{81-88}–specific CD8$^+$ T cells. The mAb therapy can exhibit immunostimulatory effects through the Fc portion of a mAb (7, 8). We investigated whether the augmented antitumor effect by combination treatment depended on the Fc portion of the mAb. BALB/c mice bearing CT26-NY-ESO-1 tumors were injected with 5-FU (days 7 and 14) and intact antibody or an Fc-depleted form of the anti-NY-ESO-1 mAb (days 9 and 16). The antitumor effect induced by the combination treatment with the intact anti-NY-ESO-1 mAb and 5-FU was totally abolished when F(ab) antibodies were administered (Fig. 5A). We further examined the critical role of the Fc portion for this augmented antitumor effect by the combination treatment using activating Fcγ receptor knockout mice (Fcer1g$^{-/-}$ mice). In these mice, we did not observe the augmented antitumor effect by the combination treatment compared with mice treated with 5-FU alone (Fig. 5B), confirming the critical role of the antibody–Fc portion for this augmented antitumor effect.

Accumulation of antibody to tumor sites by combination treatment

Given the importance of the Fc portion and the antigen–antibody IC formation for an enhancement of CD8$^+$ T cells

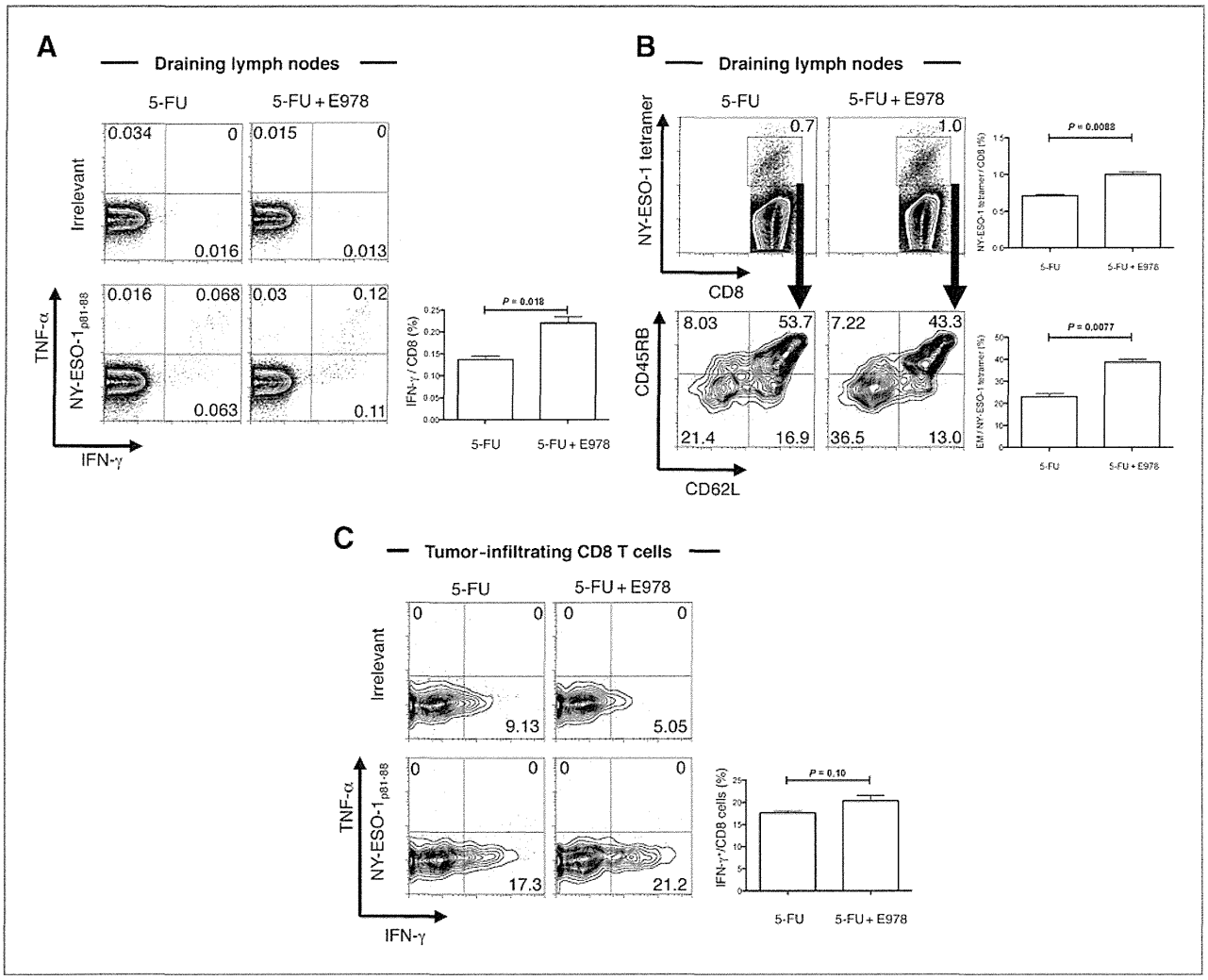

Figure 3. Combination treatment enhances NY-ESO-1–specific CD8$^+$ T-cell induction. A–C, BALB/c mice ($n = 3$) were inoculated with CT26-NY-ESO-1 and injected with 5-FU and anti-NY-ESO-1 mAb (E978). A, on day 14, dLNs were removed and incubated with NY-ESO-1_{81-88} or control peptide. IFN-γ and TNF-α secretion by CD8$^+$ T cells was analyzed. B, dLN cells were isolated on day 16, and CD45RB and CD62L expression on NY-ESO-1_{81-88}–specific CD8$^+$ T cells identified as CD8$^+$NY-ESO-1_{81-88}/D^d tetramer$^+$ T cells was analyzed. C, tumor-infiltrating lymphocytes were collected on day 16 and incubated with NY-ESO-1_{81-88} or control peptide. IFN-γ and TNF-α secretion by CD8$^+$ T cells was analyzed. These experiments were repeated twice with similar results. Data are presented as mean ± SD. EM, effector/memory T cells.

(19–21), we examined the accumulation of the anti-NY-ESO-1 mAb to tumor sites for assessing the *in vivo* formation of antigen–antibody IC. For this purpose, we used a human anti-NY-ESO-1 mAb to detect and visualize the accumulation of anti-NY-ESO-1 mAb at the tumor sites. BALB/c mice bearing CT26-NY-ESO-1 received 5-FU and human anti-NY-ESO-1 mAb 2 days later. Tumors were removed several time points after the mAb injection. Anti-NY-ESO-1 mAb accumulated in CT26-NY-ESO-1 tumors after 24 hours and maintained thereafter when given in combination with 5-FU (Fig. 6A and B). In contrast, the accumulation of anti-NY-ESO-1 mAb in the tumors was lower without 5-FU treatment (Fig. 6A and B). We next tested whether the released NY-ESO-1 protein localized around the area of 5-FU–induced cell death. Anti-NY-ESO-1 mAb accumulated around the apoptotic area detected by cleaved caspase-3 staining (Fig. 6B), suggesting that 5-FU accentuated the natural release of intracellular NY-ESO-1 from dying tumor cells subsequently resulting in an increased accumulation of anti-NY-ESO-1 mAb in tumors and the formation of antigen–antibody IC.

Formation of antigen–antibody IC *in vivo* by the combination treatment induces sufficient maturation of dendritic cells for tumor eradication

We next analyzed the role of dendritic cells (DC) for this augmentation of antitumor effects. The activation status (CD80, CD86, MHC class II, and CD40) of CD11c$^+$ DCs at dLN after treatment was examined. The expression level of CD80, CD86, MHC class II, and CD40 in DCs was significantly enhanced in mice that received the combination treatment with anti-NY-ESO-1 mAb and 5-FU compared with mice treated with 5-FU alone (Fig. 6C).

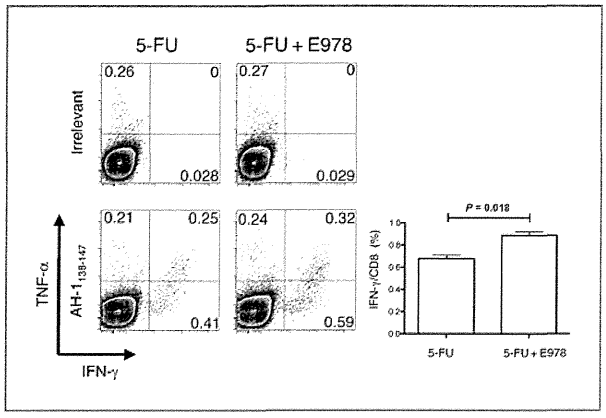

Figure 4. Antigen spreading is observed in mice that received the combination treatment. BALB/c mice ($n = 3$) were inoculated with CT26-NY-ESO-1 and injected with 5-FU and anti-NY-ESO-1 mAb (E978). On day 24, dLNs were removed and incubated with AH-$1_{138–147}$ or control peptide. IFN-γ and TNF-α secretion by $CD8^+$ T cells was analyzed. These experiments were repeated twice with similar results. Data are presented as mean ± SD.

Discussion

In view of the recent clinical successes of targeted mAbs to tumor antigens expressed on the surface of tumors for cancer therapy (3–5), we explored the feasibility to extend this approach of targeted mAb therapy to intracellular molecules as the majority of tumor antigens identified to date, are exclusively expressed and located inside the cell (14–16). Appropriate maneuvers that facilitate access of mAbs to these intracellular antigenic targets are critical requirement for this approach. Nucleoside analogues, such as 5-FU, predominantly induce apoptosis in target cells (31), but we found that NY-ESO-1 protein was released from tumor cells after 5-FU treatment in similar amounts as released by necrosis. The injected mAb accumulated into CT26-NY-ESO-1 tumors, suggesting the *in vivo* formation of antigen–antibody ICs. Furthermore, DCs in dLN that captured these ICs exhibited a mature phenotype and were associated with the induction of higher numbers of NY-ESO-1–specific $CD8^+$ T cells. This augmented antitumor immunity by combination treatment with anti-NY-ESO-1 mAb, and 5-FU was abrogated in nude mice and wild-type mice depleted of $CD8^+$ cells, arguing that a major involvement of ADCC or complement is less likely. Furthermore, this augmented antitumor effect by intracellular antigen-specific mAb combined with chemotherapy was observed in another tumor system using doxorubicin, indicating the broader application of this combination treatment.

A combination of anti-Her2 mAb and HER2/neu-expressing granulocyte macrophage colony-stimulating factor (GM-CSF)-secreting tumor vaccine augmented the antitumor effect compared with either treatment alone, and the improved therapeutic efficacy was dependent on Fc-mediated activation of APCs (11). TA-99 (recognizing Trp1) mAb enhanced DNA vaccination–induced antitumor effects (12). More recently, Park and colleagues showed that the therapeutic effect of an

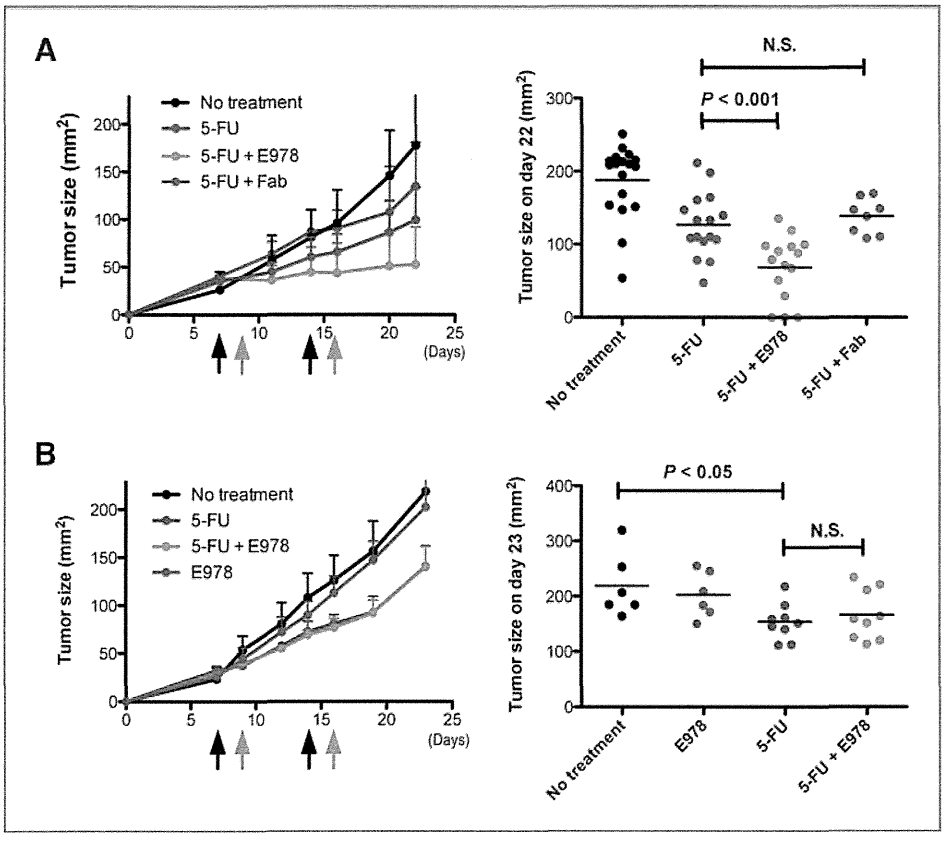

Figure 5. The Fc receptor signals are required for augmented antitumor effects by the combination treatment. A, BALB/c mice were inoculated with CT26-NY-ESO-1 and injected with 5-FU (days 7 and 14) and intact or Fc-depleted F(ab) anti-NY-ESO-1 mAb (E978, days 9 and 16). B, Fcγ receptor knockout mice were inoculated with CT26-NY-ESO-1 and injected with 5-FU (days 7 and 14) and anti-NY-ESO-1 mAb (E978, days 9 and 16). Tumor size was monitored 3 times a week. Each group consisted of 3 to 10 mice. Left, tumor growth curves representative of 2 independent experiments; right, summary of tumor size of 2 independent experiments on day 22 (A) and day 23 (B). Data are presented as mean ± SD. N.S., not significant.

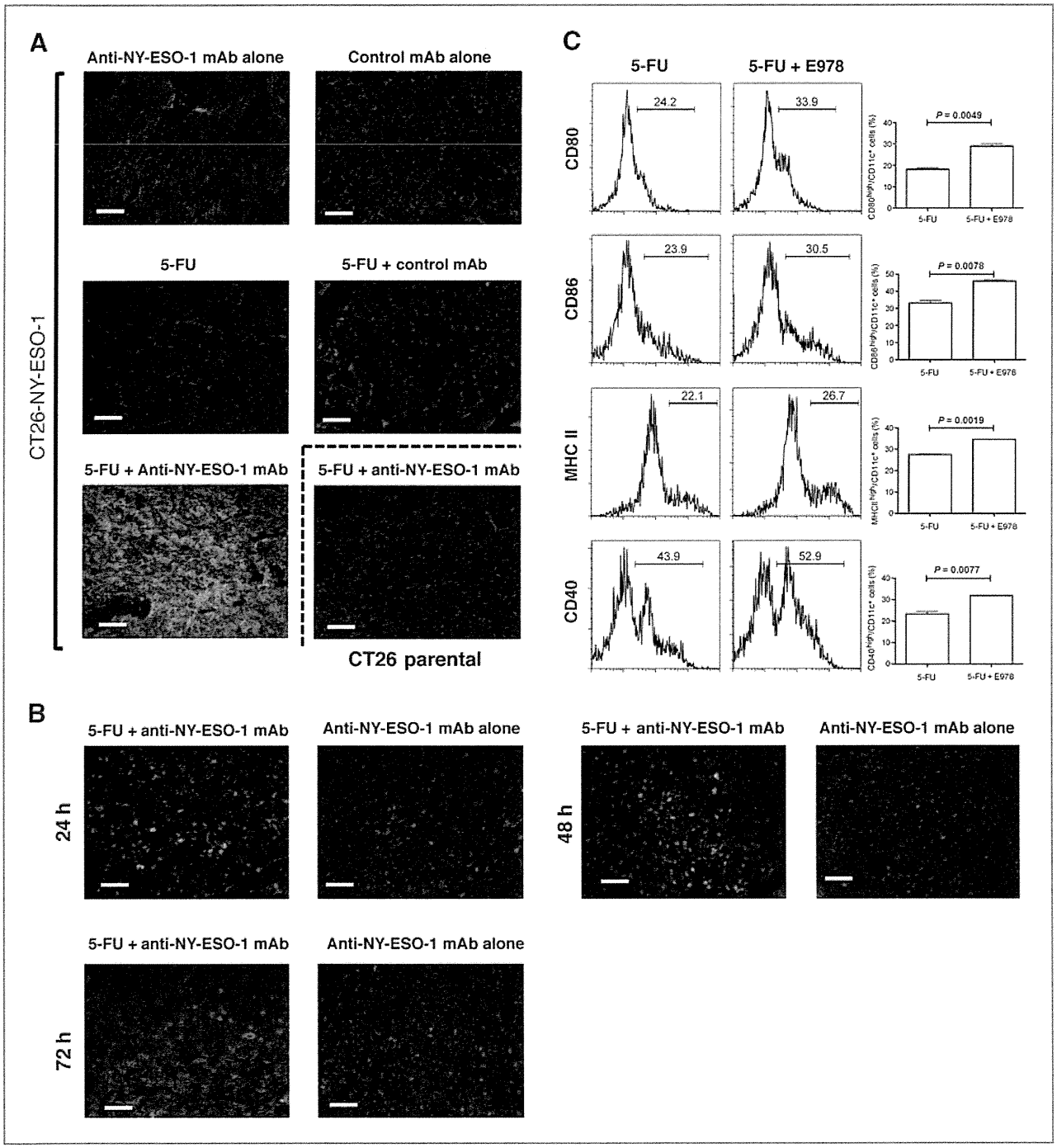

Figure 6. The combination treatment results in accumulation of injected antibody at the tumor site and induces maturation of DCs. A, BALB/c mice were inoculated with CT26-NY-ESO-1 and injected with 5-FU (day 5) and human anti-NY-ESO-1 mAb (12D7, day 7) or human anti-A33 mAb as a control (day 7). Twenty-four hours after mAb injection, tumors were removed and the accumulation of human anti-NY-ESO-1 mAb into tumors was examined by immunohistochemistry. Bar, 50 mm). B, CT26-NY-ESO-1 tumors as in A were removed at the indicated time points after mAb injection and costained with antihuman IgG mAb (green) and anti-cleaved caspase-3 mAb (red). Bar, 50 μm. C, two days after the last 5-FU injection, dLNs were harvested. CD80, CD86, CD40, and MHC class II expression on $CD11c^{high}$ DCs was analyzed. These experiments were repeated twice with similar results.

anti-HER2/neu mAb was associated with adaptive cellular immune responses, such as $CD8^+$ T cells (13). While these data clearly implicated a critical role for Fc-mediated APC activation and cross-priming correlated with enhancement of antigen-specific $CD8^+$ T-cell induction, other or additional mechanisms may include direct signal blocking and other Fc-mediated antitumor effects as the target antigens were expressed on the cell surface. These data, therefore, do not

unambiguously suggest a possible application of mAb therapy to intracellular molecules. Here, we show that Fc-mediated antigen-specific $CD8^+$ T-cell induction was an important element of mAb therapy using mAbs against tumor antigens that are exclusively expressed in the intracellular compartment and we suggest the potential application of targeted mAb therapy also to intracellular tumor antigens. As a result, it is of interest to readdress the correlation between antitumor effect of $CD8^+$ T-cell response and clinical response by trastuzumab (anti-Her2/neu) treatment, as trastuzumab is able to enhance cross-presentation *in vitro* (32).

Another unique point in our study is that our mAb treatment targeting an intracellular antigen does not require *in vitro* formation of IC or a combination with antigen immunization, such as protein or DNA vaccines for the formation of antigen–antibody IC (10–12, 33). When the mAb was injected alone, an augmented antitumor effect was not observed in our model, suggesting the essential role of chemotherapy for releasing sufficient amounts of antigen to form antigen–antibody IC. Other modalities for facilitating antigen release from tumors, such as radiation therapy, cryoablation, or other agents, that may result in partial destruction of tumor cells could be applicable to this combination therapy. These results are particularly important for considering the clinical application of targeted mAb therapy because combination of chemotherapy and mAbs have already been widely used in the clinic (3–5). Furthermore, combining a mAb therapy with protein or DNA cancer vaccines is very expensive and enormous effort is required to translate into the clinic.

$CD4^+$ T cell help is necessary for a proper activation and a long-lasting memory formation of $CD8^+$ T cells (34, 35). While combination treatment with anti-NY-ESO-1 mAb and chemotherapy provided an augmented antitumor efficacy and induced higher numbers of NY-ESO-1–specific $CD8^+$ T cells with effector/memory type, these effects were dependent on $CD8^+$ T cells but not $CD4^+$ T cells. One can envisage that as a major role of $CD4^+$ T cells is to stimulate APCs, such as DCs, to activate $CD8^+$ T cells (licensing; refs. 34, 35), signals provided through Fc receptors may compensate the $CD4^+$ T-cell help for stimulating/activating APCs. Alternatively, inflammation induced by anticancer drugs further supports the stimulating/activating of APCs.

One intriguing question is why the combination of mAb and 5-FU exhibited a strong antitumor effect, despite a possible inhibitory signal through a subclass of IgG, namely, IgG1 used in this study (8). Because we used anti-NY-ESO-1 mAbs (mouse IgG1) for this combination therapy, IgG1 may show inhibitory function by activating inhibitory Fc receptor (7–9). Some protocols of anticancer chemotherapy induce the stimulation of immune responses by Toll-like receptor ligands released from tumor cells (36). The possibility that 5-FU–induced tumor destruction stimulates inflammation signals, such as Toll-like receptor signals, and these inflammation signals may change the ratio of stimulatory/inhibitory Fc receptor expression to a more stimulatory condition (8) is less likely because our preliminary data show that the balance between activating Fcγ receptor III and inhibitory Fcγ receptor IIB expression on $CD11c^+$ cells was not influenced by 5-FU treatment. This raises several possibilities as follows: (i) the balance between those receptors changes on other hematopoietic cells, (ii) signaling pathways through those Fcγ receptors are altered by chemotherapy-induced inflammation, and (iii) antibody specificity is not good enough to address this point and proper knockout animals are required. In addition, it will be crucial to compare the effect of immunologic responses by other IgG subclasses, and studies with class-switched antibodies and with Fcγ receptor IIB knockout mice are planned.

We observed that mAb and 5-FU combination treatment resulted in the development of an immune response against tumor antigens that have not been directly targeted by the antibody but that are expressed in tumor cells, a phenomenon known as antigen spreading (22, 29, 30). While mice treated with 5-FU alone or without treatment elicited NY-ESO-1–specific $CD8^+$ T-cell responses, antigen spreading and its therapeutic effectiveness were limited in these mice. It is also possible that efficient activation of DCs by the targeted mAb and 5-FU combination treatment provides the opportunity to stimulate subsequently additional $CD8^+$ T cells specific for other antigens derived from the tumor cells. Therefore, effective antitumor responses, such as tumor eradication, may require $CD8^+$ T cells specific for the single antigen used for immunization but also multiple antigens that were contained in tumors, as shown in other murine systems and human cancer vaccines (1, 22, 37, 38).

In our model as well as in patients with cancer, NY-ESO-1 humoral responses could be spontaneously elicited. While a correlation between humoral responses and longer survival was not reported, NY-ESO-1–specific $CD8^+$ T-cell induction by cross-priming *in vivo* is associated with the induction of specific antibodies (2, 39). Spontaneous NY-ESO-1 humoral responses are correlated with progression of tumor stage in humans (2, 39). In our mouse system, spontaneously induced anti-NY-ESO-1 antibodies were observed when tumors reached a larger size. The level of spontaneously induced antibodies is about 10 times lower than that achieved by mAb injection (Supplementary Fig. S1C), suggesting that spontaneously induced humoral responses may potentially have some antitumor effects, but the amount of antibodies may be too low to exhibit effective antitumor activity, such as facilitating tumor regression. Our data revealed that mAb and 5-FU combination treatment induced higher numbers of effector/memory NY-ESO-1–specific $CD8^+$ T cells than by chemotherapy alone, reflecting a long-lasting antitumor capacity as shown by improved survival. In conclusion, combination treatment with targeted mAbs and chemotherapy opens a new era of antibody cancer immunotherapy for tumor antigens with intracellular expression.

Disclosure of Potential Conflicts of Interest

No potential conflicts of interests were disclosed.

Authors' Contributions

Conception and design: T. Noguchi, T. Kato, A. Knuth, S. Gnjatic, G. Ritter, L.J. Old, H. Shiku, H. Nishikawa

Development of methodology: T. Noguchi, H. Ikeda, E. Sato, A. Knuth, G. Ritter, L.J. Old
Acquisition of data (provided animals, acquired and managed patients, provided facilities, etc.): T. Noguchi, G. Ritter
Analysis and interpretation of data (e.g., statistical analysis, biostatistics, computational analysis): T. Noguchi, T. Kato, Y. Maeda, S. Gnjatic, G. Ritter, L.J. Old, H. Shiku, H. Nishikawa
Writing, review, and/or revision of the manuscript: T. Noguchi, T. Kato, H. Ikeda, A. Knuth, S. Gnjatic, G. Ritter, S. Sakaguchi, L.J. Old, H. Shiku, H. Nishikawa
Administrative, technical, or material support (i.e., reporting or organizing data, constructing databases): T. Noguchi, L. Wang, H. Ikeda, G. Ritter, S. Sakaguchi
Study supervision: T. Kato, G. Ritter, L.J. Old, H. Shiku

In Memoriam

This article is dedicated to the memory of L.J. Old.

Acknowledgments

The authors thank the contribution of the late Dr. S. Kondo for discussion. The authors also thank Drs. T. Takahashi, M. van den Broek, and J. Wing for critical reading of the manuscript and M. Yamane for technical assistance.

Grant Support

This study was supported by Grants-in-Aid for Scientific Research (B; no. 23300354 to H. Nishikawa), the Cancer Research Institute Investigator Award (H. Nishikawa) and Cancer Vaccine Collaborative Grant for Immunological Monitoring (S. Gnjatic, G. Ritter, and L.J. Old), Cancer Research Grant from Foundation of Cancer Research Promotion (H. Nishikawa), and Atlantic Philanthropies (G. Ritter, L.J. Old).

The costs of publication of this article were defrayed in part by the payment of page charges. This article must therefore be hereby marked *advertisement* in accordance with 18 U.S.C. Section 1734 solely to indicate this fact.

Received September 15, 2011; revised December 27, 2011; accepted January 18, 2012; published OnlineFirst February 8, 2012.

References

1. Boon T, Coulie PG, Van den Eynde BJ, van der Bruggen P. Human T cell responses against melanoma. Annu Rev Immunol 2006;24:175–208.
2. Gnjatic S, Nishikawa H, Jungbluth AA, Gure AO, Ritter G, Jager E, et al. NY-ESO-1: review of an immunogenic tumor antigen. Adv Cancer Res 2006;95:1–30.
3. Dougan M, Dranoff G. Immune therapy for cancer. Annu Rev Immunol 2009;27:83–117.
4. Coiffier B, Lepage E, Briere J, Herbrecht R, Tilly H, Bouabdallah R, et al. CHOP chemotherapy plus rituximab compared with CHOP alone in elderly patients with diffuse large-B-cell lymphoma. N Engl J Med 2002;346:235–42.
5. Hudis CA. Trastuzumab–mechanism of action and use in clinical practice. N Engl J Med 2007;357:39–51.
6. Regnault A, Lankar D, Lacabanne V, Rodriguez A, Thery C, Rescigno M, et al. Fcγ receptor-mediated induction of dendritic cell maturation and major histocompatibility complex class I-restricted antigen presentation after immune complex internalization. J Exp Med 1999;189:371–80.
7. Nimmerjahn F, Ravetch JV. Divergent immunoglobulin g subclass activity through selective Fc receptor binding. Science 2005;310:1510–2.
8. Nimmerjahn F, Ravetch JV. Fcγ receptors as regulators of immune responses. Nat Rev Immunol 2008;8:34–47.
9. Clynes RA, Towers TL, Presta LG, Ravetch JV. Inhibitory Fc receptors modulate *in vivo* cytotoxicity against tumor targets. Nat Med 2000;6:443–6.
10. Wolpoe ME, Lutz ER, Ercolini AM, Murata S, Ivie SE, Garrett ES, et al. HER-2/neu-specific monoclonal antibodies collaborate with HER-2/neu-targeted granulocyte macrophage colony-stimulating factor secreting whole cell vaccination to augment $CD8^+$ T cell effector function and tumor-free survival in Her-2/neu-transgenic mice. J Immunol 2003;171:2161–9.
11. Kim PS, Armstrong TD, Song H, Wolpoe ME, Weiss V, Manning EA, et al. Antibody association with HER-2/neu-targeted vaccine enhances $CD8^+$ T cell responses in mice through Fc-mediated activation of DCs. J Clin Invest 2008;118:1700–11.
12. Saenger YM, Li Y, Chiou KC, Chan B, Rizzuto G, Terzulli SL, et al. Improved tumor immunity using anti-tyrosinase related protein-1 monoclonal antibody combined with DNA vaccines in murine melanoma. Cancer Res 2008;68:9884–91.
13. Park S, Jiang ZJ, Mortenson ED, Deng LF, Radkevich-Brown O, Yang XM, et al. The therapeutic effect of anti-HER2/neu antibody depends on both innate and adaptive immunity. Cancer Cell 2010;18:160–70.
14. Kawakami Y, Rosenberg SA. Human tumor antigens recognized by T-cells. Immunol Res 1997;16:313–39.
15. Old LJ, Chen Y-T. New paths in human cancer serology. J Exp Med 1998;187:1163–7.
16. Simpson AJ, Caballero OL, Jungbluth A, Chen YT, Old LJ. Cancer/testis antigens, gametogenesis and cancer. Nat Rev Cancer 2005;5:615–25.
17. Hara I, Takechi Y, Houghton AN. Implicating a role for immune recognition of self in tumor rejection: passive immunization against the brown locus protein. J Exp Med 1995;182:1609–14.
18. Chen YT, Scanlan MJ, Sahin U, Tureci O, Gure AO, Tsang S, et al. A testicular antigen aberrantly expressed in human cancers detected by autologous antibody screening. Proc Natl Acad Sci U S A 1997;94:1914–8.
19. Dhodapkar KM, Krasovsky J, Williamson B, Dhodapkar MV. Antitumor monoclonal antibodies enhance cross-presentation of cellular antigens and the generation of myeloma-specific killer T cells by dendritic cells. J Exp Med 2002;195:125–33.
20. Nagata Y, Ono S, Matsuo M, Gnjatic S, Valmori D, Ritter G, et al. Differential presentation of a soluble exogenous tumor antigen, NY-ESO-1, by distinct human dendritic cell populations. Proc Natl Acad Sci U S A 2002;99:10629–34.
21. Valmori D, Souleimanian NE, Tosello V, Bhardwaj N, Adams S, O'Neill D, et al. Vaccination with NY-ESO-1 protein and CpG in Montanide induces integrated antibody/Th1 responses and CD8 T cells through cross-priming. Proc Natl Acad Sci U S A 2007;104:8947–52.
22. Nishikawa H, Sato E, Briones G, Chen LM, Matsuo M, Nagata Y, et al. *In vivo* antigen delivery by a *Salmonella typhimurium* type III secretion system for therapeutic cancer vaccines. J Clin Invest 2006;116:1946–54.
23. Muraoka D, Kato T, Wang LA, Maeda Y, Noguchi T, Harada N, et al. Peptide vaccine induces enhanced tumor growth associated with apoptosis induction in $CD8^+$ T cells. J Immunol 2010;185:3768–76.
24. Griswold DP, Corbett TH. A colon tumor model for anticancer agent evaluation. Cancer 1975;36:2441–4.
25. Ikeda H, Ohta N, Furukawa K, Miyazaki H, Wang L, Kuribayashi K, et al. Mutated mitogen-activated protein kinase: a tumor rejection antigen of mouse sarcoma. Proc Natl Acad Sci U S A 1997;94:6375–9.
26. Stockert E, Jager E, Chen Y-T, Scanlan MJ, Gout I, Karbach J, et al. A survey of the humoral immune response of cancer patients to a panel of human tumor antigens. J Exp Med 1998;187:1349–54.
27. Nagata Y, Furugen R, Hiasa A, Ikeda H, Ohta N, Furukawa K, et al. Peptides derived from a wild-type murine proto-oncogene c-*erb*B-2/HER2/*neu* can induce CTL and tumor suppression in syngeneic hosts. J Immunol 1997;159:1336–43.
28. Huang AY, Gulden PH, Woods AS, Thomas MC, Tong CD, Wang W, et al. The immunodominant major histocompatibility complex class I-restricted antigen of a murine colon tumor derives from an endogenous retroviral gene product. Proc Natl Acad Sci U S A 1996;93:9730–5.
29. Lehmann PV, Forsthuber T, Miller A, Sercarz EE. Spreading of T-cell autoimmunity to cryptic determinants of an autoantigen. Nature 1992;358:155–7.
30. Vanderlugt CL, Miller SD. Epitope spreading in immune-mediated diseases: implications for immunotherapy. Nat Rev Immunol 2002;2:85–95.
31. Sampath D, Rao VA, Plunkett W. Mechanisms of apoptosis induction by nucleoside analogs. Oncogene 2003;22:9063–74.
32. Kono K, Sato E, Naganuma H, Takahashi A, Mimura K, Nukui H, et al. Trastuzumab (Herceptin) enhances class I-restricted antigen

presentation recognized by HER-2/neu-specific T cytotoxic lymphocytes. Clin Cancer Res 2004;10:2538–44.
33. Rafiq K, Bergtold A, Clynes R. Immune complex-mediated antigen presentation induces tumor immunity. J Clin Invest 2002;110:71–9.
34. Kennedy R, Celis E. Multiple roles for $CD4^+$ T cells in anti-tumor immune responses. Immunol Rev 2008;222:129–44.
35. Arens R, Schoenberger SP. Plasticity in programming of effector and memory $CD8^+$T-cell formation. Immunol Rev 2010;235:190–205.
36. Apetoh L, Ghiringhelli F, Tesniere A, Obeid M, Ortiz C, Criollo A, et al. Toll-like receptor 4-dependent contribution of the immune system to anticancer chemotherapy and radiotherapy. Nat Med 2007;13:1050–9.
37. Germeau C, Ma WB, Schiavetti F, Lurquin C, Henry E, Vigneron N, et al. High frequency of antitumor T cells in the blood of melanoma patients before and after vaccination with tumor antigens. J Exp Med 2005;201:241–8.
38. Lurquin C, Lethe B, De Plaen E, Corbiere V, Theate I, van Baren N, et al. Contrasting frequencies of antitumor and anti-vaccine T cells in metastases of a melanoma patient vaccinated with a MAGE tumor antigen. J Exp Med 2005;201:249–57.
39. Gure AO, Chua R, Williamson B, Gonen M, Ferrera CA, Gnjatic S, et al. Cancer-testis genes are coordinately expressed and are markers of poor outcome in non-small cell lung cancer. Clin Cancer Res 2005;11:8055–62.